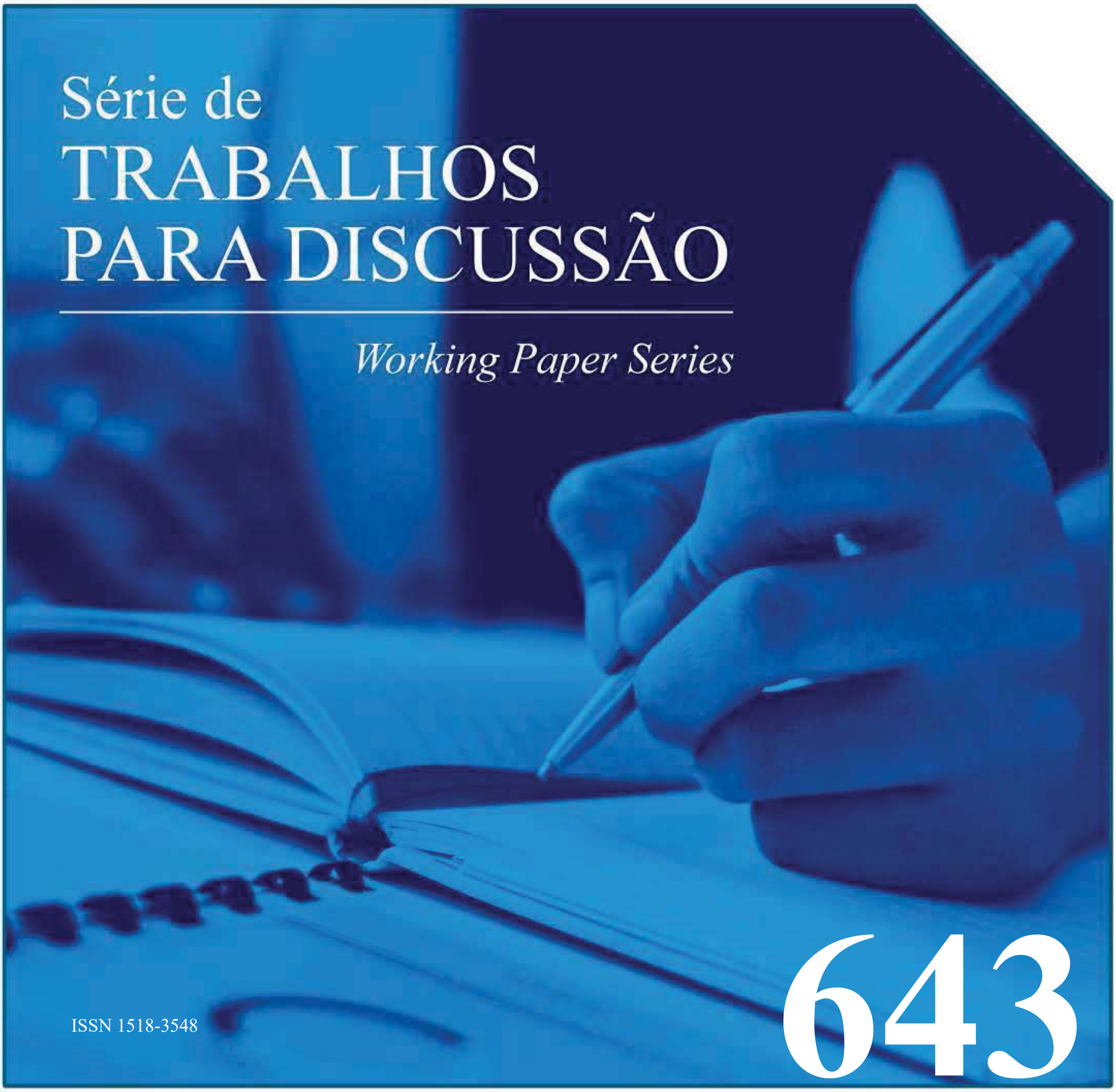

Abril 2026

Beating the "Pros" with a Semi-structural Model of their own Inflation Forecasts

Sergio Lago Alves, Waldyr Areosa, Carlos Carvalho

BANCO CENTRAL DO BRASIL

ISSN 1518-3548
CGC 00.038.166/0001-05

Working Paper Series	Brasília	no. 643	Abril	2026	p. 3-48

Working Paper Series

Edited by the Research Department (Depep) – E-mail: workingpaper@bcb.gov.br

Editor: Rodrigo Barbone Gonzalez

Co-editor: Eurilton Alves Araujo Jr

Head of the Research Department: Euler Pereira Gonçalves de Mello

Deputy Governor for Economic Policy: Paulo Picchetti

Citizen Service Division

Banco Central do Brasil

Deati/Diate

SBS – Quadra 3 – Bloco B – Edifício-Sede – 2º subsolo

70074-900 Brasília – DF – Brazil

Toll Free: 0800 9792345

Fax: +55 (61) 3414-2553

Internet: http//www.bcb.gov.br/?CONTACTUS

Non-Technical Summary

We address the challenge of improving inflation forecasts by leveraging the information contained in professionals' inflation forecasts. Even though being hard to beat, the literature has shown these forecasts are subject to information frictions.

And so, explicitly modeling the sources of forecast rigidity should allow one to extract the relevant information contained in reported forecasts and improve upon them. For that, we use a semi-structural model to describe the inflation process, decomposing it into trend and cycle. And rather than treating survey forecasts as rational, we explicitely model them as being subject to horizon-specific forecast rigidity.

For inference, we consider a mixed-frequency data, comprised by monthly non-seasonally adjusted US CPI inflation and quarterly forecasts from the US Survey of Professional Forecasters (SPF) as observables. We estimate the model using Monte Carlo methods. We find our model's enhanced nowcasts strongly and significantly beat SPF, with mean squared errors 50% smaller than those implied by SPF average forecasts. For the remaining horizons, our forecasts are at par with SPF survey.

The model also provides a detailed decomposition of inflation into trend and cycle components. This decomposition reveals the recent surge in US inflation is primarily driven by medium-run components rather than permanent trend inflation. This insight is crucial for policymakers who need to distinguish between transitory and persistent inflationary pressures.

Lastly, in order to shed light on the underlying reasons why we significantly outperform average SPF inflation nowcasts, we build upon a simple theoretical model of noisy-dispersed information to show the model outperforms average professional forecasts when disagreement among individual forecasters is sufficiently large.

Sumário Não-Técnico

Abordamos o desafio de melhorar as previsões de inflação alavancando as informações contidas nas previsões profissionais de inflação. Embora sejam difíceis de superar, a literatura mostra que previsões profissionais estão sujeitas a fricções de informação.

E assim, modelar explicitamente as fontes de rigidez de previsão deve permitir extrair informação relevante contida nas previsões profissionais e melhorá-las. Para isso, usamos um modelo semiestrutural para descrever o processo de inflação, decompondo-o em tendência e ciclo. E em vez de tratar as previsões profissionais como racionais, as modelamos explicitamente como sujeitas à rigidez de previsão específica por horizonte.

Para inferência, consideramos dados com frequência mista, compostos por inflação mensal não ajustada sazonalmente do IPC dos EUA e previsões trimestrais da Pesquisa de Previsores Profissionais dos EUA (SPF) como observáveis. Estimamos o modelo usando métodos de Monte Carlo. Descobrimos que os *nowcasts* aprimorados (para o trimestre corrente) do nosso modelo superam forte e significativamente o SPF, com erros quadráticos médios 50% menores do que aqueles implícitos nas previsões médias do SPF. Para os horizontes restantes, nossas previsões estão em pé de igualdade com a pesquisa do SPF.

O modelo também fornece uma decomposição detalhada da inflação em componentes de tendência e ciclo. Essa decomposição revela que o aumento recente na inflação dos EUA foi impulsionado principalmente por componentes de médio prazo, em vez de inflação de longo prazo. Esse insight é crucial para formuladores de políticas que precisam distinguir entre pressões inflacionárias transitórias e persistentes.

Por fim, para lançar luz sobre as razões subjacentes pelas quais superamos significativamente as previsões de inflação médias do SPF, construímos um modelo teórico simples de informações dispersas com ruído para mostrar que o modelo supera as previsões profissionais médias quando a discordância entre os analistas individuais é suficientemente grande.

Beating the "Pros" with a Semi-structural Model of their own Inflation Forecasts*

Sergio Lago Alves
Bank of Canada

Waldyr Areosa
Banco Central do Brasil
and PUC-Rio

Carlos Carvalho
Kapitalo Investimentos
and PUC-Rio

March 25, 2026

Abstract

Professional inflation forecasts contain valuable information but exhibit information frictions. We extract improved forecasts by explicitly modeling these frictions using US Survey of Professional Forecasters data, and find that forecast rigidity increases systematically with horizon, rising from near zero for backcasts to 0.81 beyond two quarters. In pseudo-real-time tests, our Resetting Nowcasts reduce mean squared errors by 50 percent relative to SPF averages. We derive a novel theoretical criterion showing that improved forecasts dominate when disagreement lies within an optimal interval determined by simple sufficient statistics, easily computable from any survey microdata. The criterion determines in advance the horizons where improved forecasts should dominate, without estimating friction parameters. This generalizes easily to other surveys and variables, providing a tractable, method for identifying which forecast horizons offer the greatest potential for improvement.

JEL Codes: C53, E31, E37, C11

Keywords: survey expectations, information frictions, forecast disagreement, inflation forecasting and nowcasting

*For comments and suggestions we thank Olivier Coibion, Mike West, Oleksiy Kryvtsov, Roberto Billi, Tatjana Dahlhaus, Rodrigo Sekkel, Luis Uzeda, Kerem Tuzcuoglu, Elena Goldman and participants at the 2024 CEBRA Conference, 2023 NBER-NSF SBIES Conference, and seminars at Bank of Canada and Carleton University. The views expressed in this paper are those of the authors and do not necessarily reflect the views of Bank of Canada nor Banco Central do Brasil. E-mails: slagoalves@bank-banque-canada.ca, waldyr.dutra@bcb.gov.br, cvianac@econ.puc-rio.br.

1 Introduction

Monetary policy operates with long and uncertain lags, requiring policymakers to distinguish persistent from transitory inflation movements. Survey-based inflation expectations from professional forecasters provide valuable signals beyond headline inflation, as these analysts incorporate diverse data sources using models and judgment, and their collective forecasts are difficult to outperform in accuracy (e.g. Faust and Wright (2013)).[1] Yet extensive research documents that such forecasts exhibit information frictions rather than strict rationality (e.g. Coibion and Gorodnichenko (2015)).[2] This raises a fundamental question: can modeling these frictions extract the useful information embedded in professional forecasts and improve upon them?

We answer affirmatively firstly by performing an empirical exercise, based on estimating a model of forecast frictions, to extract useful information embedded in professionals' forecasts — what we call *Resetting Forecasts* —, showing that they strongly outperform US Survey of Professional Forecasters (SPF) consensus nowcasts, released by the Federal Reserve Bank of Philadelphia. Secondly, we provide a tractable theoretical framework to show that forecast disagreement is key in determining whether Resetting Forecasts dominate survey aggregates. Building on a model of noisy-dispersed information, we derive an optimal interval for disagreement: it must be sufficiently large to signal meaningful information dispersion, but not so large that forecasts become unreliable. The importance of this novel theoretical criterion is that it does not depend on estimating a model of forecast frictions. The optimal interval depends only on three sufficient statistics — unconditional variance of individual forecast errors, unconditional variance of average forecast errors, and unconditional variance of inflation —, which can be inferred from any survey dataset. This criterion correctly predicts the horizons where our empirical approach succeeds. And impotantly, this theoretical tool is generalizable to other surveys and forecasted varfiables, allowing for easier ex-ante identification of horizons with the greatest potential for improvement.

The empirical exercise uses a semi-structural state-space model that decomposes inflation into trend and cycle components using both the inflation time series and the term structure of SPF ex-

[1] Faust and Wright (2013) find that survey-based forecasts, such as Blue Chip and the SPF, outperform model-based forecasts, often by a wide margin. As Del Negro and Eusepi (2011) emphasize, professional forecasters have richer information sets that yield more precise readings of economic conditions. See also Ang, Bekaert, and Wei (2007), Croushore (2010), Faust and Wright (2009), Aiolfi, Capistran, and Timmermann (2012), Rossi and Sekhposyan (2015), and Knotek II and Zaman (2017).

[2] See, among others, Mankiw and Reis (2002), Woodford (2003), Sims (2003), Mackowiak and Wiederholt (2009), Patton and Timmermann (2010), Patton and Timmermann (2011), Andrade and Le Bihan (2013), Coibion and Gorodnichenko (2012), Coibion and Gorodnichenko (2015), and Andrade, Crump, Eusepi, and Moench (2016).

pectations.[3] The model incorporates information frictions that vary by forecast horizon—a feature we show is essential for forecast accuracy. This approach yields three main contributions. First, we find that forecast rigidity increases systematically with horizon length, rising from essentially zero for backcasts to 0.81 beyond the two-quarters-ahead horizon. Models imposing uniform rigidity across horizons are strongly rejected by the data. This finding extends Coibion and Gorodnichenko (2015) by documenting substantial heterogeneity in information frictions across the term structure of expectations. Second, we establish that properly modeling these horizon-specific frictions enables significant improvements in forecast accuracy. In pseudo out-of-sample tests over 2006-2023, our quarterly Resetting Nowcasts dominate SPF averages, reducing mean squared errors by approximately 50 percent, with statistical significance under both Giacomini and White (2006) and Diebold and Mariano (1995) tests. At longer horizons, performance is comparable, consistent with theoretical predictions we develop. Third, our inflation decomposition also provides policy-relevant insights. We find that only a small portion of the 2021-2023 US inflation surge reflected permanent shifts in trend inflation. Most reflected medium-run transitory components, a finding with important implications for the appropriate monetary policy response.

Methodologically, we estimate a mixed-frequency state-space model combining monthly non-seasonally adjusted CPI data with quarterly SPF forecasts spanning backcasts through four-quarter-ahead projections. Using non-seasonally adjusted CPI data avoids complications from dealing with vintage revisions. And so, we explicitly model time-varying seasonality in the state-space model. The model nests a rational-forecaster benchmark and specifications with both uniform and horizon-varying rigidity parameters.

Our work relates to several strands of literature. Nason and Smith (2013) and Mertens and Nason (2018) also model forecast frictions and survey term structures but impose uniform rigidity and do not test forecast improvements. Jain (2018) examines SPF individual forecasts through the lens of loss aversion but finds no performance gains. Monti (2010) augments a DSGE model with judgmental forecasts to improve fit, whereas we use survey information to enhance estimation of the inflation process itself. More broadly, our approach connects to work extracting signals from cross-sectional forecast disagreement and to research on optimal forecast combination under model uncertainty.

[3] This follows the traditional literature on trend inflation and trend-cycle decompositions in the spirit of Beveridge and Nelson (1981), applied to inflation analyses by Stock and Watson (2007, 2010) and Schmitt-Grohe and Uribe (2022), among others.

In short, our paper makes three key contributions. First, we show that explicitly modeling information frictions in professional inflation forecasts allows one to extract the underlying signals and improve upon reported forecasts. Second, we demonstrate that forecast frictions are horizon-specific and that accounting for this heterogeneity significantly enhances nowcasting and short-horizon forecasting accuracy. Third, we provide a simple theoretical criterion, based on readily available sufficient statistics, that identifies the horizons where improved forecasts are likely to dominate survey aggregates, offering a tractable and generalizable tool for analyzing survey expectations beyond the SPF.

The remainder of the paper proceeds as follows. Section 2 presents the model and characterizes SPF information sets.Section 3 describes data and estimation. Section 4 reports forecast performance tests. Section 5 develops the theory of forecast dominance. Section 6 concludes.

2 Modelling Strategy

For reasons better explained further on, we consider a rich model with mixed frequency to account for observed monthly non-seasonally adjusted CPI inflation and quarterly SPF forecasts. Despite the fact that most of the literature works with pure quarterly data when dealing with SPF forecasts, the way quarterly CPI inflation is computed suggests that the most appropriate frequency to model the underlying inflation data-generating process is monthly. Following, we elaborate on the reasons for this choice.

SPF forecasts for CPI inflation aims at average-price inflation rates, i.e. the growth rate of the arithmetic mean of all three monthly CPI indexes in the quarter. If one wants to work with a linear state-space model, then we must obtain a log-linear approximation of this definition (see Section 2.2). As Mariano and Murasawa (2003) and Dahlhaus, Guenette, and Vasishtha (2017) show for any generic variables, the (linearized) definition implies a mapping from five lagged monthly rates into the average-index rates in a way that it is impossible to account for when using pure quarterly data. That is, the mapping assigns different, but symmetric, weights on five months: the last two months from the previous quarter and all three months from the current quarter.

Therefore, on the one hand, the very nature of the average-price inflation rates requires dealing with a monthly frequency model for inflation. On the other hand, SPF forecasts are realized in a quarterly frequency. Therefore, a mixed-frequency framework seems more appropriate.

An important inference strategy we adopt is that we do not observe seasonally adjusted inflation rates, and so we opt to use non-seasonally adjusted CPI rates. This choice is due to the fact that seasonally adjusted inflation is subject to revisions. And so, if we were to observe that variable in inference exercises, we would always need adjust the vintage available to forecasters in each period of time. In the literature, this adjustment is always discretionary, varying from author to author, and generates questions on how old (or recent) the appropriate vintage must be in each quarter.[4]

In order to cope with seasonally adjusted inflation rates, we include an internal filter based on Harrison and West (1997, chap. 8.2-8.4) and Harrison and Stevens (1975). This state-space modelling is able to extract time-varying seasonal patterns.

In the remainder of this section, we describe our model. In the mixed-frequency context, we represent monthly periods with t, in order to distinguish them from quarterly periods q.

2.1 The Inflation Data-Generating Process

The DGP for (logarithmic) monthly aggregate CPI inflation, non-seasonally adjusted, comprises four components that are unobserved to the econometrician: (i) a long-run (lr) persistent (unit root) trend component, π_t^{lr}; (ii) a medium-run (mr) transitory component, π_t^{mr}; (iii) a short-run (sr) transitory component π_t^{sr}; and (iv) a time-varying seasonal component, π_t^{sea}.[5] Denoting aggregate inflation by π_t, we have:

$$\pi_t = \pi_t^{sea} + \pi_t^{sr} + \pi_t^{mr} + \pi_t^{lr}. \tag{1}$$

Indeed, as shown in Section 3.2, US CPI data strongly and significantly supports the existence of two transitory components with different frequencies. In this sense, the two transitory components are allowed to have AR(1) dynamics, in which the inertial parameter of π_t^{sr} is smaller than that

[4] For instance, Coibion and Gorodnichenko (2015) use real-time values available one year after the relevant time horizon. Faust and Wright (2013) use the real-time dataset of the Federal Reserve Bank of Philadelphia, recorded two quarters after the quarter to which the data refer. Lastly, Knotek II and Zaman (2017) treat the third monthly estimate of CPI prices as "truth," as registered in the St. Louis Fed's Archival Federal Reserve Economic Data (ALFRED).

[5] Following the tradition in assessing frictions in professional forecasts, we consider a reduced form structure for the inflation data generating process (DGP). For instance, Coibion and Gorodnichenko (2015) consider a reduced-form AR(1) process for a macroeconomic variable in order to derive their noisy-information model for forecast rigidity. In the light of the Lucas critique, we assume professional forecasters fully incorporate policy-implied dynamics into their best forecasts. Therefore, the flaws caused by Lucas (1976) critique will be greatly minimized when the estimated model is augmented with professional forecasts after correctly modelling their frictions structure.

of π_t^{mr}, in absolute value:

$$\begin{aligned} \pi_t^{sr} &= \rho_{sr}\pi_{t-1}^{sr} + \varepsilon_t^{sr} \quad &; \ \varepsilon_t^{sr} \sim N\left(0, \sigma_{sr}^2\right), \\ \pi_t^{mr} &= \rho_{mr}\pi_{t-1}^{mr} + \varepsilon_t^{mr} \quad &; \ \varepsilon_t^{mr} \sim N\left(0, \sigma_{mr}^2\right), \end{aligned} \tag{2}$$

where $|\rho_{sr}| < |\rho_{mr}| < 1$.

Long-run or trend inflation, π_t^{lr}, follows a random-walk, thus contributing for a loose-end level for inflation:

$$\pi_t^{lr} = \pi_{t-1}^{lr} + \varepsilon_t^{lr} \quad ; \ \varepsilon_t^{lr} \sim N\left(0, \sigma_{lr}^2\right). \tag{3}$$

Indeed, Cogley and Sbordone (2008) and Faust and Wright (2013) highlight the importance to account for slow-moving changes in trend inflation (local means) for forecast purposes.[6]

Defining the (logarithmic) seasonally adjusted monthly inflation rate π_t^{sa} is also key when dealing with information coming from surveys:

$$\pi_t^{sa} \equiv \pi_t - \pi_t^{sea} = \pi_t^{mr} + \pi_t^{sr} + \pi_t^{lr} \tag{4}$$

Note that our approach is in line with Faust and Wright (2013) forecasting principles. In particular, they find good forecasts must account for a slowly varying non-stationary trend inflation π_t^{lr} and model the inflation gap $\pi_t^{gap} \equiv \left(\pi_t^{sa} - \pi_t^{lr}\right)$ as a stationary component. In our specification, the inflation gap is accounted by $(\pi_t^{mr} + \pi_t^{sr})$, whose stationarity is ensured by the parameter restrictions $|\rho_{mr}| < 1$ and $|\rho_{sr}| < 1$.[7]

Lastly, a time-varying seasonal component, π_t^{sea}, allows the model to capture changes in seasonal patterns due to reasons such as a smoothly evolving inflation seasonality pattern, or abruptly

[6] In particular, Faust and Wright (2013) also consider a random walk formulation for trend inflation in one of their models.

[7] We can easily derive the dynamics of this component as $\left(\pi_t^{hpr} + \pi_t^{lpr}\right) = \left(\rho_{hpr} + \rho_{lpr}\right)\left(\pi_{t-1}^{hpr} + \pi_{t-1}^{lpr}\right) - \rho_{hpr}\rho_{lpr}\left(\pi_{t-2}^{hpr} + \pi_{t-2}^{lpr}\right) + \varepsilon_t^{hpr} + \varepsilon_t^{lpr} - \rho_{lpr}\varepsilon_{t-1}^{hpr} - \rho_{hpr}\varepsilon_{t-1}^{lpr}$. Therefore, stability requires $\rho_{lpr}\rho_{hpr} < 1$, $\left(\rho_{lpr} + \rho_{hpr}\right) < \left(1 + \rho_{lpr}\rho_{hpr}\right)$, and $\left(\rho_{lpr} + \rho_{hpr}\right) > -\left(1 + \rho_{lpr}\rho_{hpr}\right)$. Provided that $\left|\rho_{hpr}\right| < 1$, note that $\left(\rho_{lpr} + \rho_{hpr}\right) < \left(1 + \rho_{lpr}\rho_{hpr}\right)$ implies $\rho_{lpr} < 1$, and $\left(\rho_{lpr} + \rho_{hpr}\right) > -\left(1 + \rho_{lpr}\rho_{hpr}\right)$ implies $\rho_{lpr} > -1$. Therefore, $\left|\rho_{hpr}\right| < 1$ and $\left|\rho_{lpr}\right| < 1$ are sufficient to ensure stationarity of $\left(\pi_t^{hpr} + \pi_t^{lpr}\right)$.

changes in the methodology for computing the consumption price index:

$$
\begin{aligned}
\pi_t^{sea} &= \pi_{1,t}^{sea}, \\
\pi_{1,t}^{sea} &= \pi_{2,t-1}^{sea} - \bar{\pi}_{t-1}^{sea} + \varepsilon_t^{sea} \qquad\qquad ; \; \varepsilon_t^{sea} \sim N\left(0, \sigma_{sea}^2\right) \\
\pi_{2,t}^{sea} &= \pi_{3,t-1}^{sea} - \bar{\pi}_{t-1}^{sea} - \tfrac{1}{T_y-1}\varepsilon_t^{sea}, \\
&\vdots \\
\pi_{T_y,t}^{sea} &= \pi_{1,t-1}^{sea} - \bar{\pi}_{t-1}^{sea} - \tfrac{1}{T_y-1}\varepsilon_t^{sea}, \\
\bar{\pi}_t^{sea} &\equiv \tfrac{1}{T_y}\textstyle\sum_{s=1}^{T_y} \pi_{s,t}^{sea}.
\end{aligned}
\tag{5}
$$

where T_y is the number of periods in a year ($T_y = 12$ for monthly frequency).

This approach to model a time-varying seasonal pattern closely follows the suggestions of Harrison and West (1997, chap. 8.2-8.4). By adding ε_t^{sea} to $\pi_{1,t}^{sea}$, subtracting $\frac{1}{T_y-1}\varepsilon_t^{sea}$ from the remaining seasonal terms (see e.g. Harrison and Stevens (1975)) and subtracting the average seasonal component $\bar{\pi}_{t-1}^{sea}$ from all seasonal terms, we ensure the average $\bar{\pi}_t^{sea}$ is always zero.

All four DGP shocks ε_t^{sr}, ε_t^{mr}, ε_t^{lr} and ε_t^{sea} hit the economy at the beginning of month t. Even though the inflation DGP process may provide information to identify those shocks, the inference process also benefits from using extra information coming from professional forecasts. They can be particularly useful if available for multiple forecasting horizons, for revisions to the term structure of inflation forecasts provide valuable information about how forecasters perceive shocks to the inflation process. In response to shocks deemed transitory, survey participants revise their short-run forecasts, but leave those for longer horizons relatively unchanged. In contrast, shocks deemed persistent affect the whole term structure of inflation forecasts. Therefore, we assess the forecast formation process in the following section.

2.2 Forecasts and Information Sets

In the Survey of Professional Forecasters (SPF),[8] respondents provide quarterly forecasts for a set of economic quantities every second month of each quarter. Initially, since 1968, the survey was conducted by the American Statistical Association and the National Bureau of Economic Research. Beginning in the third quarter of 1990, the Federal Reserve Bank of Philadelphia took over the survey and adjusted its collecting dates in order to make sure respondents' information

[8] See more details in Croushore and Stark (2019).

sets are updated with information concerning the previous quarter. SPF forecasts are collected and made public in the second month of each quarter (*pivot month*, henceforth), before monthly statistics of the first month of the quarter are released by the Bureau of Labor Statistics (BLS) and U.S. Bureau of Economic Analysis (BEA). For monthly variables, therefore, the information set is updated up to the third month of the previous quarter.

Based on the Consumer Price Index (CPI) inflation compiled by the BLS, respondents provide forecasts on seasonally adjusted quarterly measures of the average-price rate for six horizons, i.e. the previous quarter (backcast), current quarter (nowcast) and future quarters up to four quarters ahead. In each quarter q, the quarterly average-price index P_q^{av} is defined as the arithmetic mean of all three monthly CPI indexes in the quarter, i.e. $P_q^{av} \equiv \frac{1}{3}(P_{1,q} + P_{2,q} + P_{3,q})$. Therefore, the (gross) average-price rate is defined as $\Pi_q^{av} \equiv P_q^{av}/P_{q-1}^{av}$. Respondents also provide annual end-of-year measures for the current year, as well as for up to two years ahead.

In the beginning of the pivot month, respondents observe inflation with a 2-month delay. While the non-seasonally adjusted rate is final, as the BLS does not revise it, respondents only observe the first vintage of the most recent seasonally adjusted rates. Indeed, seasonally adjusted values are subject to revisions as new inflation information is released and seasonal patterns are updated. Therefore, it makes sense for the SPF to ask respondents to provide their best assessment of the previous-quarter seasonally adjusted CPI inflation rate, as respondents are trying to infer its final values after all revisions are carried out.

In order to work with such SPF idiosyncrasies, we need to address two important points. The first one regards frequency conventions, as SPF forecasts are quarterly and CPI inflation rates are monthly. The second point deals with the information set when modeling forecasts rigidity, considering what is observed by respondents when they provide forecasts.

As for the average-price variation issue, careful considerations come in handy. Considering the monthly frequency, let P_t^{sa} denote the true (not observed) seasonally adjusted CPI price index in each month. The monthly seasonally adjusted CPI (gross) inflation Π_t^{sa} is computed as $\Pi_t^{sa} = P_t^{sa}/P_{t-1}^{sa}$. If t is the pivot month, the seasonally adjusted (gross) quarterly average-price rate Π_t^{av} is computed as $\Pi_t^{av} = P_t^{av}/P_{t-3}^{av}$, where $P_t^{av} = \frac{1}{3}\left(P_{t+1}^{sa} + P_t^{sa} + P_{t-1}^{sa}\right)$. We aim to obtain a log-linearized mapping between $\Pi_t^{av}$and Π_t^{sa}. For that, lower case variables correspond to log-linearized versions of the original upper case variables, e.g. $\varkappa_t \equiv \log(\mathcal{X}_t)$. As shown in the appendix, this relation is:[9]

$$\pi_t^{av} \approx \frac{1}{3}\left[\pi_{t+1}^{sa} + 2\pi_t^{sa} + 3\pi_{t-1}^{sa} + 2\pi_{t-2}^{sa} + \pi_{t-3}^{sa}\right]$$

In what follows, we differentiate what respondents report from expectations formed conditional on their information sets, which in turn is also different from rational expectations. The latter is achieved only under perfect and complete information sets. Following, we start by describing the information sets before assessing how reported forecasts are produced.

2.2.1 Information Sets

Due to the delay in releasing monthly inflation rates π_t by the statistical agency, respondents only observe the history of inflation up to month $(t-2)$ when reporting to SPF. That is, at the pivot month they only observe inflation up to the last month of previous quarter.

In addition, we reasonably assume respondents might gather extra soft or hard public information between $(t-2)$ and right before π_{t-1} is released in period t and make better conditional assessments of π_{t-1}^{sa} and π_t^{sa}. Let s_{t-1} and s_t summarize the extra public information gathered by specialists at periods $t-1$ and t. This includes recent economic developments, specific information contained in other price indices that might have been released during this period, high-frequency analyses, and, importantly, information about future inflation developments.[10] These pieces of information allow forecasters an informed view of whether recent inflation developments are more transient or more persistent. Finally, we also assume s_t does not bring any extra information once π_t is released.

Now, we define two information sets. The first one is the full and updated information set $\mathcal{I}_t \equiv [\mathcal{I}_{t-1}, \pi_t] = [..., \pi_{t-3}, \pi_{t-2}, \pi_{t-1}, \pi_t]$, which is not available to SPF respondents. As highlighted in Monti (2010), respondents actually have access to partial information sets $\mathcal{I}_t^* \equiv \left[\mathcal{I}_{t-1}^*, \pi_{t-2}, s_t\right] = [..., \pi_{t-3}, \pi_{t-2}, s_{t-1}, s_t]$, as they observe inflation realized up to month $(t-2)$ and collects intra-quarter soft or hard information, as mentioned before.[11] Therefore, partial information sets satisfy

[9] This approximation is about the same as the one made by Mariano and Murasawa (2003) and Dahlhaus, Guenette, and Vasishtha (2017). It also has the same intuition as in Crump, Eusepi, Lucca, and Moench (2014), when they map quarterly growth rates into annual growth measures, i.e. there are triangle-shaped weights for five different months. Since t is the pivot month, the five weights peak at the first month of each quarter $(t-1)$, but span from the second month of previous quarter $(t-3)$ to the third month of current quarter $(t+1)$.

[10] This information may stem from the evolution of the general macroeconomic outlook, from announcements regarding future economic policies, and from news regarding pricing of large firms, including state-owned and regulated firms whose prices or pricing policies are frequently defined and announced in advance.

[11] Paralleling Monti (2010), the information sets $\mathcal{I}_t^*$ are partial as they satisfy $\mathcal{I}_{t-2} \subset \mathcal{I}_t^* \subset \mathcal{I}_t$.

$\mathcal{I}_t^* = [\mathcal{I}_{t-2}, \mathcal{S}_t]$, where $\mathcal{S}_t = [s_{t-1}, s_t]$ represents the extra information gathered at periods $(t-1)$ and t.

Averaging across all individual forecasts, conditional on current partial information set $\mathcal{I}_t^*$ available to respondents, we define quarterly and monthly *Resetting Forecasts* as $E_t^* \pi_{t+h}^{av} \equiv E\left(\pi_{t+h}^{av} | \mathcal{I}_t^*\right)$ and $E_t^* \pi_{t+j}^{sa} \equiv E\left(\pi_{t+j}^{sa} | \mathcal{I}_t^*\right)$, where monthly horizons $j \in \{-1, 0, 1, 2, 3, ...\}$ are not necessarily coincident with SPF horizons $h \in \{-3, 0, 3, 6, 9, 12\}$. Likewise, conditional on the last full information set $\mathcal{I}_{t-2}$, we define quarterly and monthly expectations $E_{t-2} \pi_{t+h}^{av} \equiv E\left(\pi_{t+h}^{av} | \mathcal{I}_{t-2}\right)$ and $E_{t-2} \pi_{t+j}^{sa} \equiv E\left(\pi_{t+j}^{sa} | \mathcal{I}_{t-2}\right)$.

Let $\mathfrak{s}_{j,t}$ denote a non-observed variable capturing any information in $\mathcal{S}_t$, orthogonal to $\mathcal{I}_{t-2}$, satisfying

$$E_t^* \pi_{t+j}^{sa} = E_{t-2} \pi_{t+j}^{sa} + \mathfrak{s}_{j,t} \tag{6}$$

Since $\mathcal{I}_t^* = [\mathcal{I}_{t-2}, \mathcal{S}_t]$, we obtain an important result using iterating expectations. It allows us to conclude that $E_t^* \pi_{t+j}^{sa}$ is centered around $E_{t-2} \pi_{t+j}^{sa}$ over time:

$$\begin{aligned} \int_{\mathcal{S}} E_t^* \pi_{t+j}^{sa} dP\left(\mathcal{S}_t\right) &\overset{definition}{=} \int_{\mathcal{S}} E\left(\pi_{t+j}^{sa} | \mathcal{I}_t^*\right) dP\left(\mathcal{S}_t\right) \overset{definition}{=} \int_{\mathcal{S}} E\left(\pi_{t+j}^{sa} | \mathcal{I}_{t-2}, \mathcal{S}_t\right) dP\left(\mathcal{S}_t\right) \\ &= \int_{\mathcal{S}} E\left(\pi_{t+j}^{sa} | \mathcal{I}_{t-2}, \mathcal{S}_t\right) P\left(\mathcal{S}_t\right) d\mathcal{S} = E\left(\pi_{t+j}^{sa} | \mathcal{I}_{t-2}\right) = E_{t-2} \pi_{t+j}^{sa} \end{aligned}$$

Since $\int_{\mathcal{S}} E_t^* \pi_{t+j}^{sa} dP\left(\mathcal{S}_t\right) = E_{t-2} \pi_{t+j}^{sa}$, equation (6) implies $\mathfrak{s}_{j,t}$ is unconditionally zero-meaned, i.e. $E\left(\mathfrak{s}_{j,t}\right) = 0$.[12] However, conditional on specific values for forecasts at $(t-1)$ and t, $\mathfrak{s}_{j,t}$ may have non zero conditional expectation.

Using the quarterly average-price rate approximation and $E_t^* \pi_{t+j}^{sa} = E_{t-2} \pi_{t+j}^{sa} + \mathfrak{s}_{j,t}$, resetting forecasts for $h \in \{-3, 0, 3, 6, 9, 12\}$ satisfy:

$$\begin{aligned} E_t^* \pi_{t+h}^{av} &= E_{t-2} \pi_{t+h}^{av} + \mathfrak{s}_{h,t}^{av} \\ E_t^* \pi_{t+h}^{av} &\equiv \tfrac{1}{3} E_t^* \left[\pi_{t+h+1}^{sa} + 2\pi_{t+h}^{sa} + 3\pi_{t+h-1}^{sa} + 2\pi_{t+h-2}^{sa} + \pi_{t+h-3}^{sa}\right] \\ \mathfrak{s}_{h,t}^{av} &\equiv \tfrac{1}{3} \left[\mathfrak{s}_{h+1,t} + 2\mathfrak{s}_{h,t} + 3\mathfrak{s}_{h-1,t} + 2\mathfrak{s}_{h-2,t} + \mathfrak{s}_{h-3,t}\right] \end{aligned} \tag{7}$$

[12] Note that $\mathfrak{s}_{j,t}$ behaves as if it was a disturbance that perturbs the strictly rational forecast, made with information up to $(t-2)$.

2.2.2 Forecasters

We assume the existence of a unit mass of survey respondents $i \in (0,1)$ that produce professional forecasts and know the structure and parameters describing the inflation DGP (1) − (5).[13] In the pivot month (second month) of each quarter, respondents form their quarterly forecast for the average price rate at monthly horizon h, i.e. $\mathcal{F}_{i,t}\pi^{av}_{t+h}$ for $h \in \{-3, 0, 3, 6, 9, 12\}$. Even though reporting forecasts $\mathcal{F}_{i,t}\pi^{av}_{t+h}$, respondents might have private expectations that they may not necessarily release to surveys all the time.

That is, for any monthly horizon $j \in \{-1, 0, 1, 2, 3, ...\}$, we assume respondents have private monthly expectations $E^*_{i,t}\pi^{sa}_{t+j}$, which are aggregated into average quarterly expectations $E^*_{i,t}\pi^{av}_{t+h} \approx \frac{1}{3}E^*_{i,t}\left[\pi^{sa}_{t+h+1} + 2\pi^{sa}_{t+h} + 3\pi^{sa}_{t+h-1} + 2\pi^{sa}_{t+h-2} + \pi^{sa}_{t+h-3}\right]$, for each SPF horizon $h \in \{-3, 0, 3, 6, 9, 12\}$.

As for private expectations, it is enough for now to assume individual expectations are centered about Resetting Forecasts, i.e. $\int_i E^*_{i,t}\pi^{sa}_{t+j}di = E^*_t\pi^{sa}_{t+j}$ and $\int_i E^*_{i,t}\pi^{av}_{t+h}di = E^*_t\pi^{av}_{t+h}$.

2.2.3 Forecast Rigidity

The forecast rigidity we postulate are in the spirit of informational frictions models. This choice stems from the fact that the literature on noisy information (e.g. Andrade and Le Bihan (2013) and Coibion and Gorodnichenko (2015)) has shown the existence of isomorphism, or quasi-isomorphism, between dynamic equations describing forecasts in both sticky (e.g. Mankiw and Reis (2002)) and noisy information approaches.[14] In Appendix 5.1, we follow Coibion and Gorodnichenko (2015) to verify the isomorphism, but depart from them by providing theoretical grounds for horizon-specific Kalman gains in the context of a noisy-dispersed information model.

Note that, for backcasts, SPF respondents already know the final value of non-seasonally adjusted headline inflation rate from the previous quarter, and are aware of the initial BLS vintage for the seasonally adjusted inflation rate. Therefore, they are only trying to provide improved backcasts to better match the final vintage. In this sense, we expect the corresponding backcast

[13] Later on, we assume the econometrician does not know the parameters, even though she understands the structure of the inflation DGP and the way respondents eventually fail to update their forecasts.

[14] In some information models (e.g. Woodford (2003), Sims (2003), and Mackowiak and Wiederholt (2009)), in which individual forecasters obtain public and private signals to make their forecasts, Kalman recursion implies forecast dynamics whose functional form is the same as the one obtained in sticky-information models. In this isomorphism, the Kalman gain γ plays the role as $(1-\alpha)$, where α is the probability of not updating expectations in sticky-information models. For models with heterogeneous loss aversion to forecast errors, as in Capistran and Timmermann (2009a), on the other hand, Coibion and Gorodnichenko (2015) show they imply quite similar function forms, but not exactly the same, as those of sticky-information models.

rigidity parameter to be close to zero. We also reckon that, for distant horizons, forecasts are not likely to change much after all current information is realized. In a nutshell, our assumptions imply that rigidity parameters to start at about 0, increase with the forecasting horizon and eventually converge to a stable level at distant ones.

In this context, we allow for horizon-specific forecast rigidity. With horizon-specific probability $(1-\alpha_h)$, each survey participant $i \in (0,1)$ reports her Resetting Forecast for horizon h as $\mathcal{F}_{i,t}\pi^{av}_{t+h} = E^*_{i,t}\pi^{av}_{t+h}$. With probability α_h, forecasts for horizon h are not updated, i.e. $\mathcal{F}_{i,t}\pi^{av}_{t+h} = \mathcal{F}_{i,t-1}\pi^{av}_{t+h}$. Using the results shown in Section 2.2, the aggregate forecast for horizon $(t+h)$, $\mathcal{F}_t\pi^{av}_{t+h} \equiv \int_i \mathcal{F}_{i,t}\pi^{av}_{t+h}di$, evolves according to:

$$\begin{aligned}
&\mathcal{F}_t\pi^{av}_{t+h} = (1-\alpha_h)\, E^*_t\pi^{av}_{t+h} + \alpha_h\mathcal{F}_{t-3}\pi^{av}_{t+h} \\
&E^*_t\pi^{av}_{t+h} = E_{t-2}\pi^{av}_{t+h} + \mathfrak{s}^{av}_{h,t} \\
&\mathfrak{s}^{av}_{h,t} = \tfrac{1}{3}\left[\mathfrak{s}_{h+1,t} + 2\mathfrak{s}_{h,t} + 3\mathfrak{s}_{h-1,t} + 2\mathfrak{s}_{h-2,t} + \mathfrak{s}_{h-3,t}\right]
\end{aligned} \tag{8}$$

where $E^*_t\pi^{av}_{t+h} = \int_i E^*_{i,t}\pi^{av}_{t+h}di$ is the latent Resetting Forecast for horizon $(t+h)$, for $h \in \{-3,0,3,6,9,12\}$. Our assumptions can be thought as a generalization of Monti (2010) approach. The author's model is a restricted version of (8), in which all rigidity parameters α_h are set to zero.

The recursive system that describes the formation of forecasts extends into the infinite horizon, as each forecast for horizon h depends on lagged forecast for horizon $(h+3)$, i.e. $\mathcal{F}_{t-3}\pi^{av}_{t+h} = L^3\mathcal{F}_t\pi^{av}_{t+h+3}$, where $L(\cdot)$ is the lag operator. Therefore, if one is to use (8) in econometric exercises in which forecasts are observed up to monthly horizon H, the direct approach is truncating the recursion at a horizon $(H-3)$ and loose some available information. In order to cope with this issue, we show under weak assumptions that (8) at longer horizons is equivalent to an auto-contained equation system that does not depend on lagged forecasts of longer horizons.

Proposition 1 *If the degree of forecast rigidity for any horizon $h \geq H+3$ is constant, with $H \geq 0$, and there is no extra information disturbances for those longer horizons, i.e. $\alpha_h = \bar{\alpha}$ and $\mathfrak{s}^{av}_{h,t} = 0$ for $h \in \{H+3, H+6, ...\}$, then $\mathcal{F}_t\pi^{av}_{t+h}$ evolves according to an autoregressive system that does not depend on lagged forecasts for longer horizons:*

$$\begin{aligned}
\mathcal{F}_t\pi^{av}_{t+h} &= \mathcal{F}_t\pi^{amr.}_{t+h} + \mathcal{F}_t\pi^{asr}_{t+h} + \mathcal{F}_t\pi^{alr}_{t+h} \\
\textit{where} &
\end{aligned} \tag{9}$$

$$
\begin{aligned}
\mathcal{F}_t\pi_{t+h}^{amr.} &= (1-\bar{\alpha})\,E_{t-2}\pi_{t+h}^{amr} + \bar{\alpha}\,(\rho_{mr})^3\,\mathcal{F}_{t-3}\pi_{t-3+h}^{amr} \\
\mathcal{F}_t\pi_{t+h}^{asr.} &= (1-\bar{\alpha})\,E_{t-2}\pi_{t+h}^{asr} + \bar{\alpha}\,(\rho_{sr})^3\,\mathcal{F}_{t-3}\pi_{t-3+h}^{asr} \\
\mathcal{F}_t\pi_{t+h}^{alr} &= (1-\bar{\alpha})\,E_{t-2}\pi_{t+h}^{alr} + \bar{\alpha}\mathcal{F}_{t-3}\pi_{t-3+h}^{alr}
\end{aligned}
$$

$$
\begin{aligned}
\pi_{t+h}^{amr} &\equiv \tfrac{1}{3}\left[\pi_{t+h+1}^{mr} + 2\pi_{t+h}^{mr} + 3\pi_{t+h-1}^{mr} + 2\pi_{t+h-2}^{mr} + \pi_{t+h-3}^{mr}\right] \\
\pi_{t+h}^{asr} &\equiv \tfrac{1}{3}\left[\pi_{t+h+1}^{sr} + 2\pi_{t+h}^{sr} + 3\pi_{t+h-1}^{sr} + 2\pi_{t+h-2}^{sr} + \pi_{t+h-3}^{sr}\right] \\
\pi_{t+h}^{alr} &\equiv \tfrac{1}{3}\left[\pi_{t+h+1}^{lr} + 2\pi_{t+h}^{lr} + 3\pi_{t+h-1}^{lr} + 2\pi_{t+h-2}^{lr} + \pi_{t+h-3}^{lr}\right]
\end{aligned}
$$

The proof is described in the Appendix.

Regarding this result, we highlight two points. First, as mentioned before, the latent variables on the left side of the second, third and fourth equations now depend on their own lagged values, i.e. $\mathcal{F}_{t-3}\pi_{t-3+h}^{amr} = L^3\mathcal{F}_t\pi_{t+h}^{amr.}$, $\mathcal{F}_{t-3}\pi_{t-3+h}^{asr} = L^3\mathcal{F}_t\pi_{t+h}^{asr.}$ and $\mathcal{F}_{t-3}\pi_{t-3+h}^{alr} = L^3\mathcal{F}_t\pi_{t+h}^{alr}$, and not on lagged values of longer horizons. Second, the inertial parameters ρ_{mr} and ρ_{sr} of the DGP transitory components affect the dynamics of $\mathcal{F}_t\pi_{t+h}^{amr.}$ and $\mathcal{F}_t\pi_{t+h}^{asr}$.

3 Data Set and Inference

Inference exercises are carried out with a mixed frequency data set, i.e. monthly and quarterly series. We consider a sample from July 1990 to June 2023 to simultaneously estimate DGP and forecasting parameters. We begin the samples in July 1990 as it was in the third quarter of 1990 that the Federal Reserve Bank of Philadelphia took over the Survey of Professional Forecasters (SPF), adjusting the survey respondents information sets.

For the inflation metrics π_t, we only observe the monthly non-seasonally adjusted CPI inflation (US city average, All items), released by the US Bureau of Labor Statistics. For SPF quantities, we consider all six quarterly forecast means, i.e. for backcasts $\mathcal{F}_t\pi_{t-3}^{av}$, nowcasts $\mathcal{F}_t\pi_t^{av}$ and forecasts up to four quarters ahead $\mathcal{F}_t\pi_{t+h}^{av}$, for $h \in \{3, 6, 9, 12\}$. In monthly frequency, SPF forecasts time series are sparse, as we observe each realization every second month in the quarter, with two blanks between observations.[15]

Note that using SPF forecasts as additional information to estimate the DGP parameters is in line with Del Negro and Eusepi (2011), as they highlight that including professional forecasts

[15] Here, we abstract from a potential Average Forecast bias originated by frequent entry and exit of individual forecasters, as highlighted in Capistran and Timmermann (2009b). Implicitly, we are assuming the potential bias will affect both the Average Forecasts as well as the Resetting Forecast, so that forecasting performance tests will not asymmetrically favor the latter nor the former.

among the observables is a way to exploit the forecasters' richer information set.

The model deals with logarithmized quantities, observing their appropriate time-aggregation. For instance, a 1% monthly inflation rate is logarithmized into $100 \log(1.01) = 0.995$. On the other hand, since quarterly SPF forecasts are released in annualized unities, we convert them into quarterly logarithmized unities. That is, a 10% annualized quarterly SPF forecast is logarithmized into $100 \frac{\log(1.10)}{4} = 2.38$.

3.1 Inference and Estimation

As SPF forecasts are only observed in the second month of each quarter, we treat them as having missing observations in the first and third months of each quarter. Therefore, estimation is carried out with a mixed-frequency Bayesian approach, using the Kalman filter to deal with missing observations.[16] For the Kalman filter initialization, we use a diffuse filter. We employ a Metropolis-Hastings MCMC sampler, with 2 independent chains of 1 million draws, disregarding the first 50% as burn-in. The joint prior is given by the product of uniform densities, with sufficiently wide supports. In this case, support upper bounds most be large enough, so that the posterior density mimics the likelihood function. On the other hand, extremely large supports generate inefficiencies during MCMC draws. Therefore, we have to balance efficiency versus avoiding truncate the likelihood function. For inertia (ρ_{mr}, ρ_{sr}) and rigidity (α_h) parameters, we consider their natural supports bounded between 0 and 1. As for the remaining standard deviations parameters, we considered sufficiently large supports, in the non-negative space, so that posterior densities are not truncated.

In order to closely mimic information set restrictions faced by econometricians that want to improve over realized SPF forecasts in real-time, we adjust the information set for the Kalman filter in order to obtain more realistic likelihood evaluations. In each month t in the sample, the information set is updated up to current SPF forecasts $\mathcal{F}_t \pi_{t+h}^{av}$ (as well as backcasts and nowcasts) and 2-month lagged inflation realizations π_{t-2}.

We run two exercises. As detailed below, each exercise has seven model variations to test the horizon threshold from which forecast rigidity is constant. Since one of our hypothesis is that forecast rigidity is zero for backcasts ($h = -3$), the first exercise estimates those seven models

[16] See e.g. see e.g. Prado and West (2010, Section 4.3.3) and Durbin and Koopman (2012, Section 4.10) for a discussion on Kalman filtering with missing observations.

imposing the restriction $\alpha_{-3} = 0$. The second exercise considers unrestricted models, and estimates α_{-3} in each one of them. For testing whether $\alpha_{-3} = 0$ or the horizon threshold from which forecast rigidity is constant, we use the Log Marginal Likelihood (LML) statistics. Differences in LML represents logarithmized probability odds ratios.

Both exercises have the following models. The first one, which we call *Rational Forecasts (RFR)*, assumes there are no forecast rigidities, i.e. $\alpha_h = 0$ for monthly horizon $h \in \{-3, 0, 3, 6, 9, 12\}$. Note SPF forecasts have at least three different flavors, i.e. backcasts ($h = -3$), nowcasts ($h = 0$) and forecasts ($h \geq 3$). And so, it might not be reasonable to consider that forecasting rigidities are the same for all horizons. As explained in Section 2.2.3, we actually expect rigidity parameters to start at about 0, increase with the forecasting horizon and eventually converge to a stable level at distant ones.

Therefore, we consider a broader class of six models with partially stable rigidity parameters, differing only on the horizon in which forecast rigidity parameters stabilize. That is, each *Sluggish Forecasts Horizon* $\mathcal{H}$ *(*$SF_{\mathcal{H}}$*)* model, for monthly horizon $\mathcal{H} \in \{-3, 0, 3, 6, 9, 12\}$, has specific rigidity parameters α_h for near monthly horizons $h < \mathcal{H}$ and constant parameters $\alpha_h = \bar{\alpha}_{\mathcal{H}}$ for $\forall h \geq \mathcal{H}$. Note model SF_{-3} is actually a model with constant rigidity, as it has $\alpha_h = \bar{\alpha}_{-3}$ for $\forall h \geq -3$. Due to its nature, we call it the *Uniform Sluggishness (USL)* model. On the other extreme, we have model SF_{12} with specific and different rigidity parameters α_h for all SPF forecasted horizon $h \in \{-3, 0, 3, 6, 9, 12\}$. That is, forecast rigidities do not stabilize before the farthest forecasting horizon. We call it the *Full Sluggish Forecasts (FSF)* model, for it is the fully blown version of this class of forecast rigidity models. In restricted models, imposing $\alpha_{-3} = 0$, note models RFR and SF_{-3} are identical and deliver the same results as the unrestricted RFR model.

Using the Kalman filter for likelihood evaluating, we consider information sets comprising of all contemporaneous SPF forecasts $\mathcal{F}_t \pi^{av}_{t+h}$ and 2–month lagged (non-seasonally adjusted) headline inflation π_{t-2}. In the end of the day, in a T-sized sample, the filter observes $6T/3$ quarterly SPF forecasts and T monthly inflation observations, from π_{-1} to π_{T-2}.

After estimating the models, we test their in-sample and pseudo out-of-sample performances. In-sample comparisons are done using the Log Marginal Likelihood (LML) statistics. Pseudo out-of-sample performance comparisons, better explained in Section 4, are based on the models' forecast errors when compared to the SPF ones. In each model, after accounting for restrictions on α_h, we simultaneously estimate parameters for the forecasts' laws of motion $\Theta_f \equiv$

$[\alpha_{-3}, \alpha_0, \alpha_3, \alpha_6, \alpha_9, \alpha_{12}, \sigma_{\mathfrak{s}}]$ and DGP process $\Theta_d \equiv [\rho_{mr}, \rho_{sr}, \sigma_{mr}, \sigma_{sr}, \sigma_{lr}, \sigma_{sea}]$.

For inference, we use the equations describing the inflation DGP $(1-5)$ and those describing forecast rigidity processes (8) for all SPF horizons $h \in \{-3, 0, 3, 6, 9, 12\}$, and conveniently model the latent variable $\mathfrak{s}_{h,t}$ in system (8) as a white noise disturbance $\mathfrak{s}_{h,t} \sim N(0, \sigma_h^2)$. Lastly, for inference pragmatism, we need minor assumptions to simplify estimation in this mixed-frequency estimation environment, as SPF information is much more sparse than monthly information. In Appendix C, we describe those assumptions and show how they affect the estimated forecast system.

3.2 Estimates

Tables 1 and 2 show the estimated parameters, obtained in both exercises, for the forecasts' laws of motion and DGP, including their modes and 90% credible intervals, for all unrestricted models: *Rational Forecasts (RFR)*, and *Sluggish Forecasts Horizon* $\mathcal{H}$ *(*$SF_{\mathcal{H}}$*)* models, for monthly horizon $\mathcal{H} \in \{-3, 0, 3, 6, 9, 12\}$. In restricted models, imposing $\alpha_{-3} = 0$, recall that models RFR and $\text{SF}_{\text{-}3}$ are identical and deliver the same results as the unrestricted RFR model. Except for model SF_{-3}, all models imposing $\alpha_{-3} = 0$ slightly dominate their unrestricted counterparts, as suggested by their log marginal likelihood statistics. For instance, the probability odds ratio between the restricted and unrestricted SF_6 models is $\exp(6471.5 - 6471.0) = 1.6$, which implies the restricted model is over 50% more likely than the the unrestricted one.

Notice that models that impose zero forecast rigidity for all horizons (RFR) or near constant forecast rigidity (SF_{-3} and SF_0) perform much poorer than those that allows at least to backcasts, nowcasts and forecasts to have specific parameter rigidities. Indeed, the model SF_{-3} is the simplest one that splits rigidity parameters into backcasts, nowcasts and forecasts, and has a much larger LML than those of models RFR, SF_{-3} and SF_0.

The left panel of Figure 1 depicts LML statistics for each restricted model with $\alpha_{-3} = 0$. The highest LML model (SF_6) is highlighted with a red bar. In addition, the results are in line with our main hypothesis that the degree of forecast rigidity is very close to zero for backcasts, concavely increases for longer horizons, and seems to stabilize at distant horizons. The right panel of Figure 1 compares forecast rigidity parameters for Restricted (with $\alpha_{-3} = 0$) models SF_6 (black line), SF_9 (red dotted and crosses) and SF_{12} (blue dashed with circles). The panel shows rigidity parameters at the posterior mode, in addition to SF_6 90% credible intervals.

Table 1: MCMC Estimates - Testing Forecast Rigidity Stability

Restricted Models

	RFR	SF_{-3}	SF_0	SF_3	SF_6	SF_9	SF_{12}
LML	6314.5	6314.5	6380.1	6441.3	6471.5	6468.7	6469.0
α_{-3}	0	0	0	0	0	0	0
α_0	0	0	0.332 (0.30,0.37)	0.404 (0.36,0.44)	0.369 (0.31,0.42)	0.369 (0.31,0.42)	0.369 (0.310.41)
α_3	0	0	$\underline{0.332}$ (0.30,0.37)	0.746 (0.71,0.77)	0.731 (0.70,0.76)	0.734 (0.70,0.76)	0.736 (0.70,0.76)
α_6	0	0	$\underline{0.332}$ (0.30,0.37)	$\underline{0.746}$ (0.71,0.77)	0.816 (0.79,0.84)	0.821 (0.79,0.84)	0.820 (0.79,0.84)
α_9	0	0	$\underline{0.332}$ (0.30,0.37)	$\underline{0.746}$ (0.71,0.77)	$\underline{0.816}$ (0.79,0.84)	0.808 (0.78,0.83)	0.802 (0.77,0.82)
α_{12}	0	0	$\underline{0.332}$ (0.30,0.37)	$\underline{0.746}$ (0.71,0.77)	$\underline{0.816}$ (0.79,0.84)	$\underline{0.808}$ (0.78,0.83)	0.833 (0.80,0.85)
σ_{s}	0.020 (0.02,0.02)	0.020 (0.02,0.02)	0.028 (0.02,0.03)	0.065 (0.06,0.07)	0.074 (0.07,0.08)	0.073 (0.06,0.08)	0.074 (0.07,0.08)
ρ_{mr}	0.580 (0.55,0.60)	0.580 (0.55,0.60)	0.578 (0.56,0.60)	0.880 (0.84,0.90)	0.926 (0.91,0.94)	0.923 (0.90,0.94)	0.928 (0.91,0.94)
ρ_{sr}	−0.302 (−0.36,−0.24)	−0.302 (−0.36,−0.24)	−0.324 (−0.41,−0.25)	0.098 (0.01,0.17)	0.119 (0.04,0.19)	0.115 (0.04,0.19)	0.119 (0.04,0.19)
σ_{mr}	0.134 (0.12,0.15)	0.134 (0.12,0.15)	0.185 (0.17,0.21)	0.094 (0.08,0.11)	0.076 (0.06,0.09)	0.077 (0.06,0.09)	0.075 (0.06,0.09)
σ_{sr}	0.246 (0.23,0.27)	0.246 (0.23,0.27)	0.208 (0.19,0.23)	0.221 (0.20,0.24)	0.225 (0.21,0.24)	0.225 (0.21,0.24)	0.225 (0.21,0.24)
σ_{lr}	0.007 (0.01,0.01)	0.007 (0.01,0.01)	0.009 (0.01,0.01)	0.005 (0.00,0.01)	0.005 (0.00,0.01)	0.005 (0.00,0.01)	0.005 (0.00,0.01)
σ_{sea}	0.063 (0.05,0.07)	0.063 (0.05,0.07)	0.051 (0.04,0.06)	0.044 (0.03,0.06)	0.040 (0.03,0.05)	0.040 (0.03,0.05)	0.040 (0.03,0.05)

Notes: Restricted models imposing $\alpha_{-3} = 0$. The statistics are modes, 90% credible intervals and Log Marginal Likelihood (LML). Mixed frequency sample: July 1990 to June 2023. Net sample size: 1188 observations. In-sample rate of missing observations: 57.1%. Observed variables: monthly headline CPI (non-seasonally adjusted) rate, quarterly SPF backcast, nowcast, and forecasts up to 4 quarters ahead for quarterly CPI rates. Metropolis-Hastings MCMC with 2 independent chains of 1000000 draws and 50% burnin rate. Rational Forecasts (RFR) model imposes fixed $\alpha_h = 0$ for all horizons $h \geq -3$. Sluggish Forecasts Horizon $\mathcal{H}$ ($SF_{\mathcal{H}}$) models, for monthly horizon $\mathcal{H} \in \{-3, 0, 3, 6, 9, 12\}$, have specific and different rigidity parameters α_h for monthly horizons $h < \mathcal{H}$ and fixed parameters $\alpha_h = \bar{\alpha}_{\mathcal{H}}$ for all horizons $h \geq \mathcal{H}$. Underlined modes refer to fixed parameters at $h > \mathcal{H}$.

Table 2: MCMC Estimates - Testing Forecast Rigidity Stability
Unrestricted Models

	RFR	SF_{-3}	SF_0	SF_3	SF_6	SF_9	SF_{12}
LML	6314.5	6324.5	6376.3	6439.0	6471.0	6467.3	6467.8
α_{-3}	0	0.220 (0.18,0.26)	0.000 (0.00,0.03)	0.032 (0.00,0.08)	0.060 (0.00,0.11)	0.058 (0.00,0.11)	0.064 (0.00,0.11)
α_0	0	0.220 (0.18,0.26)	0.332 (0.30,0.37)	0.416 (0.37,0.46)	0.393 (0.34,0.45)	0.393 (0.33,0.45)	0.395 (0.33,0.45)
α_3	0	0.220 (0.18,0.26)	0.332 (0.30,0.37)	0.752 (0.72,0.78)	0.743 (0.71,0.77)	0.745 (0.71,0.77)	0.748 (0.71,0.78)
α_6	0	0.220 (0.18,0.26)	0.332 (0.30,0.37)	0.752 (0.72,0.78)	0.825 (0.80,0.85)	0.829 (0.80,0.85)	0.828 (0.80,0.85)
α_9	0	0.220 (0.18,0.26)	0.332 (0.30,0.37)	0.752 (0.72,0.78)	0.825 (0.80,0.85)	0.817 (0.79,0.84)	0.812 (0.78,0.83)
α_{12}	0	0.220 (0.18,0.26)	0.332 (0.30,0.37)	0.752 (0.72,0.78)	0.825 (0.80,0.85)	0.817 (0.79,0.84)	0.842 (0.81,0.86)
$\sigma_{\mathfrak{s}}$	0.020 (0.02,0.02)	0.018 (0.02,0.02)	0.028 (0.02,0.03)	0.067 (0.06,0.08)	0.078 (0.07,0.09)	0.077 (0.07,0.09)	0.078 (0.07,0.09)
ρ_{mr}	0.580 (0.55,0.60)	0.814 (0.75,0.86)	0.578 (0.56,0.60)	0.882 (0.85,0.90)	0.927 (0.91,0.94)	0.924 (0.91,0.94)	0.930 (0.91,0.94)
ρ_{sr}	−0.302 (−0.36,−0.24)	0.337 (0.25,0.40)	−0.324 (−0.41,−0.25)	0.107 (0.02,0.19)	0.134 (0.06,0.21)	0.130 (0.05,0.20)	0.135 (0.05,0.21)
σ_{mr}	0.134 (0.12,0.15)	0.052 (0.04,0.08)	0.185 (0.17,0.21)	0.095 (0.08,0.11)	0.078 (0.06,0.09)	0.079 (0.07,0.10)	0.078 (0.06,0.09)
σ_{sr}	0.246 (0.23,0.27)	0.224 (0.21,0.24)	0.208 (0.19,0.23)	0.221 (0.20,0.24)	0.225 (0.21,0.24)	0.225 (0.21,0.24)	0.225 (0.21,0.24)
σ_{lr}	0.007 (0.01,0.01)	0.006 (0.00,0.01)	0.009 (0.01,0.01)	0.005 (0.00,0.01)	0.005 (0.00,0.01)	0.005 (0.00,0.01)	0.005 (0.00,0.01)
σ_{sea}	0.063 (0.05,0.07)	0.209 (0.19,0.23)	0.051 (0.04,0.06)	0.044 (0.03,0.06)	0.040 (0.03,0.05)	0.040 (0.03,0.05)	0.040 (0.03,0.05)

Notes: Unrestricted models. The statistics are modes, 90% credible intervals and Log Marginal Likelihood (LML). Mixed frequency sample: July 1990 to June 2023. Net sample size: 1188 observations. In-sample rate of missing observations: 57.1%. Observed variables: monthly headline CPI (non-seasonally adjusted) rate, quarterly SPF backcast, nowcast, and forecasts up to 4 quarters ahead for quarterly CPI rates. Metropolis-Hastings MCMC with 2 independent chains of 1000000 draws and 50% burnin rate. Rational Forecasts (RFR) model imposes fixed $\alpha_h = 0$ for all horizons $h \geq -3$. Sluggish Forecasts Horizon $\mathcal{H}$ ($SF_{\mathcal{H}}$) models, for monthly horizon $\mathcal{H} \in \{-3, 0, 3, 6, 9, 12\}$, have specific and different rigidity parameters α_h for monthly horizons $h < \mathcal{H}$ and fixed parameters $\alpha_h = \bar{\alpha}_{\mathcal{H}}$ for all horizons $h \geq \mathcal{H}$. Underlined modes refer to fixed parameters at $h > \mathcal{H}$.

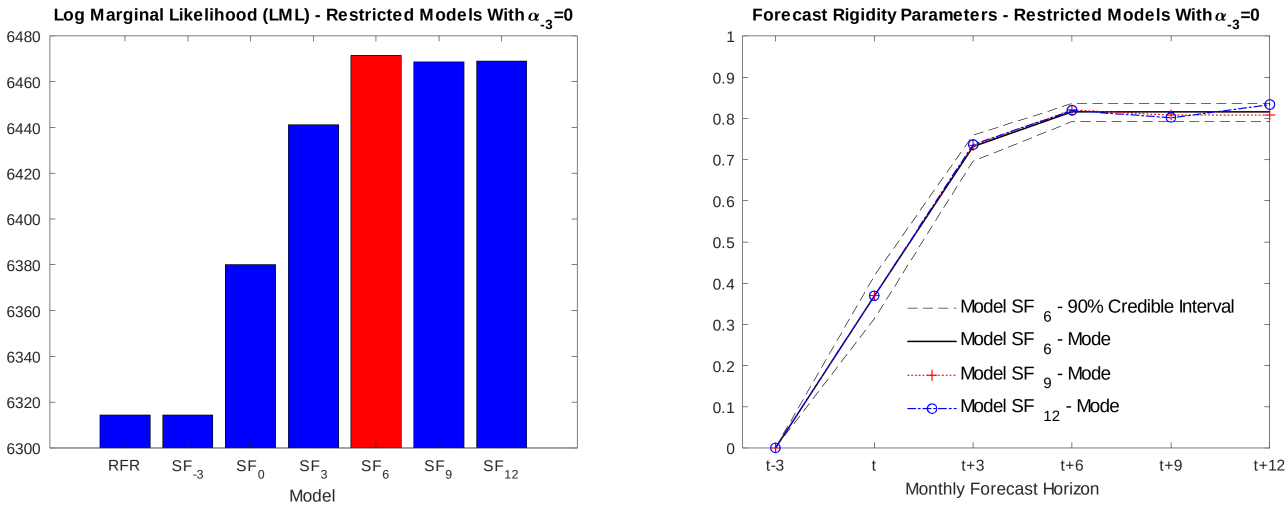

Figure 1: Testing Rigidity Stability in Forecast Horizons

Notes: LML stands for Log Marginal Likelihood. The highest LML model (SF_6) is highlighted with a red bar. Sluggish Forecasts Horizon $\mathcal{H}$ ($SF_{\mathcal{H}}$) models, for monthly horizon $\mathcal{H} \in \{-3, 0, 3, 6, 9, 12\}$, have specific and different rigidity parameters α_h for near horizons $h < \mathcal{H}$ and fixed parameters $\alpha_h = \bar{\alpha}_{\mathcal{H}}$ for all horizons $h \geq \mathcal{H}$.

Since the Restricted SF_6 model (with $\alpha_{-3} = 0$) has the largest LML statistics, we show its parameters marginal posterior density plots (black lines) in Figure 2. All parameters seem to be perfectly identified, specially when considering we use flat priors (red dashed lines). Using the Restricted SF_6 model's posterior distribution, Figure 3 shows its underlying DGP components from July 1990 to June 2023. Solid lines show inference based on mode parameters, while dotted lines show 90% credible intervals based on the parameters' asymmetric distribution.

The left panel on the top row compares the model-based long-run trend inflation to the Adjusted SPF 10-Year CPI inflation rate. Since the SPF 10-Year CPI inflation rate is meant to be the forecast for the average annual rate from current year until 10 years in the future, we compute the adjusted forecast by discounting the available forecasts for the immediately shorter horizon nearest to 10-Year ahead horizon. That is, we discount the SPF 2-Year Forecast until 2005Q1, and from 2005Q2 on, we use the SPF 5-Year forecast for discounting, adjusting the forecasts' time spams. We highlight that the Adjusted SPF 10-Year CPI inflation rate is not used as an observed variable in inference exercises, and is only shown here for comparison purposes.

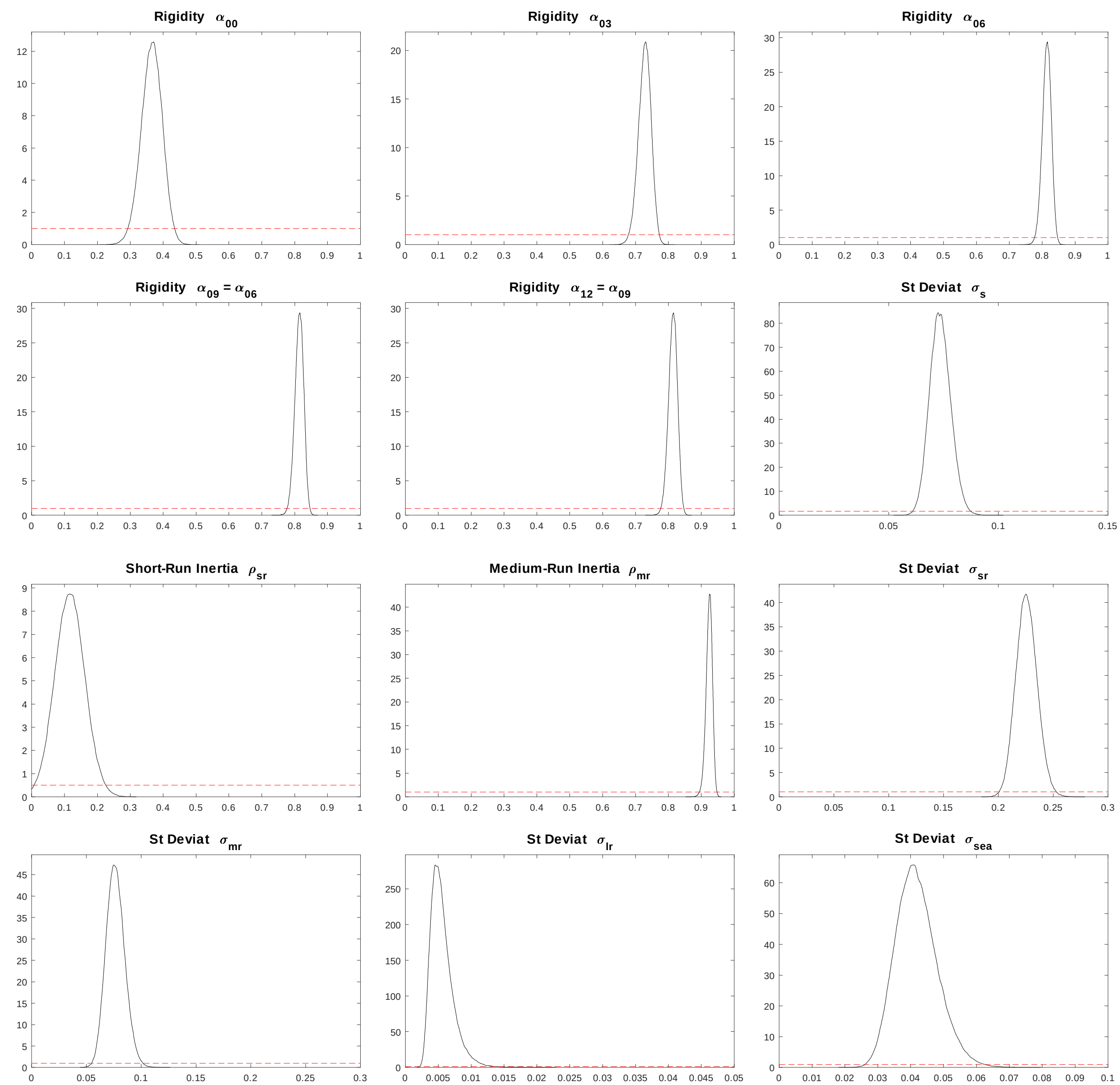

Figure 2: Density Plot - Restricted SF6 Model

Notes: SF_6 model. Marginal posterior density (black lines), Marginal prior density (red dashed lines). Metropolis-Hastings MCMC with 2 independent chains of 1000000 draws and 50% burnin rate. Mixed frequency sample: July 1990 to June 2023. Net sample size: 1188 observations. In-sample rate of missing observations: 57.1%. Observed variables: monthly headline CPI (non-seasonally adjusted) inflation rate, Quarterly SPF backcast, nowcast, and forecasts up to 4 quarters ahead for quarterly CPI inflation rates.

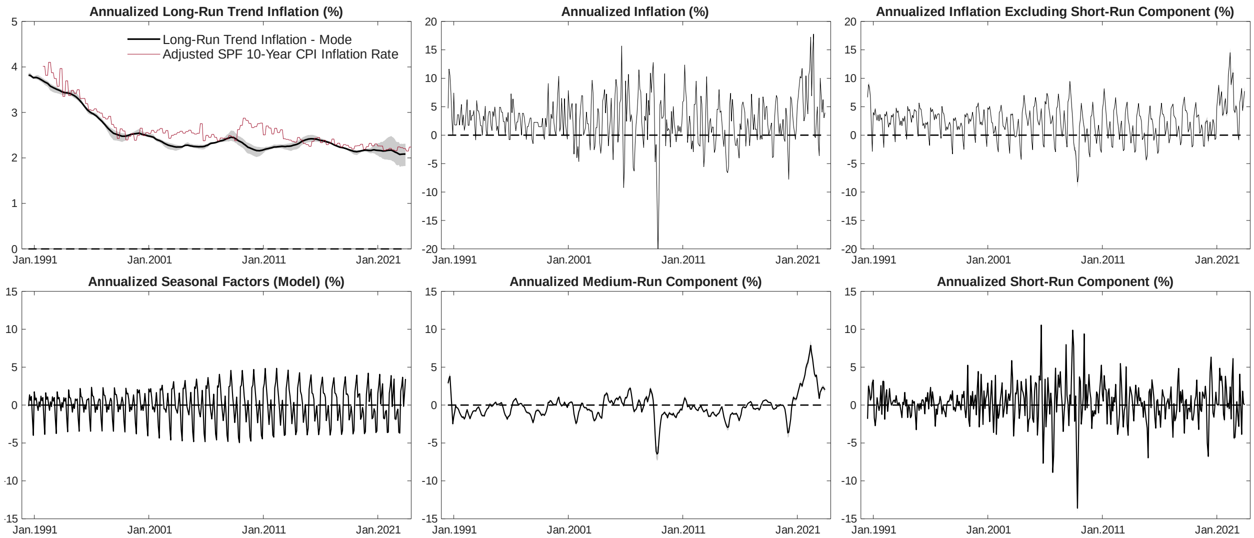

Figure 3: DGP Components - Restricted SF6 Model

Notes: SF_6 model's DGP components obtained from Kalman filter smoothed distribution, aggregated into annualized monthly frequency, from July 1990 to June 2023. Solid lines show inference based on mode parameters. Dotted lines show 90% credible intervals based on parameters' asymmetric distribution. The Adjusted SPF 10-Year CPI inflation rate was computed by discounting the SPF 2-Year Forecast (untill 2005Q1). Fom 2005Q2 on, we use the SPF 5-Year forecast for discounting. The Adjusted SPF 10-Year CPI inflation rate is not used as an observed variable in inference exercises, and is only shown here for comparison purposes.

A first thing to highlight is how stable and well-behaved the model-based long-run trend inflation has evolved, whereas the SPF 10-Year CPI inflation rate presents more erratic fluctuations. Since 2000, the model-based long rate has been stable under a 2.20-2.50 percent range. As for the stationary medium-run component, with half-life of about $\frac{\log(0.5)}{\log(0.92)} \approx 8.3$ months, the results suggest this is the one increasing since September 2020, during the inflation surge caused by the COVID-19 pandemics, while the long-rate has remained stable at a 2.30 percent level. The stationary short-run component, with half-life of about $\frac{\log(0.5)}{\log(0.12)} \approx 0.3$ months, became slightly more volatile since the pandemics stroke, but not as strongly as it was during the world financial crisis.

Also notice the Kalman filter interprets a sizeable share of inflation fluctuations as short-run components. In fact, as shown in the right panel on the top row, it is much easier to visually identify trends, transitory components and the seasonal pattern after excluding the short-run component. This task is not that easy for the full non-seasonally adjusted inflation rate, depicted in the middle panel on the top row. As for the time-varying seasonal pattern, the model seems to do a good job to endogenously capture its evolution. This result is important, as we do not observe seasonally adjusted CPI inflation in inference exercises.

In Schmitt-Grohe and Uribe (2022), the authors do not decompose transitory inflation components into short and medium run and do not use forecast data. They find that the only way to obtain a stable long-run component post COVID-19 and attribute the major fraction of observed post COVID-19 inflation to transitory components is to expand the sample to include the first half of the 20th century. Using postwar data, their model interprets the recent inflation surge as mostly coming from long-run components. In our model, we do not need to use such a large sample to obtain the same conclusion. With our approach, on the other hand, we only use data starting from July 1990 on and still manage to find a stable long-run component and attribute the recent inflation surge to transitory components.

4 Forecast Performance

As one of our main goals is to obtain relevant information to improve forecast accuracy, we now proceed to a simple comparison between SPF Average Forecasts $\mathcal{F}_t \pi^{av}_{t+h}$, for all horizons $h \in \{-3, 0, 3, 6, 9, 12\}$, against model-based pseudo out-of-sample Resetting Forecasts $E^*_t \pi^{av}_{t+h}$. In Section 5, we proof a proposition on forecasting performance, showing the necessary theoretical conditions for Resetting Forecasts to dominate Average Forecasts.

We start from model forecasts of logarithmized monthly rates $E^*_t \pi^{sa}_{t+j} = E_{t-2} \pi^{sa}_{t+j} + \mathfrak{s}_{j,t}$, and build the annualized rates in levels. As explained in Section 2.2, the extra terms $\mathfrak{s}_{j,t}$ are not simple econometrics error terms, for they convey intra-quarter soft and higher frequency information, i.e. information in $\mathcal{S}_t$, orthogonal to $\mathcal{I}_{t-2}$. As we find in this section, $\mathfrak{s}_{j,t}$ is a key forecast component for nowcasts. Even though we find $E_{t-2} \pi^{sa}_{t+j}$ nowcasting performance is somehow better than that of pure SPF nowcasts, $E^*_t \pi^{sa}_{t+j}$ is strongly and significantly better than SPF nowcasts. As the results suggest, $\mathfrak{s}_{j,t}$ adds important nowcasting value into $E^*_t \pi^{sa}_{t+j}$.

Note that the logarithmized forecasts' laws of motion (8), i.e. $\mathcal{F}_t \pi^{av}_{t+h} = (1 - \alpha_h) E^*_t \pi^{av}_{t+h} + \alpha_h \mathcal{F}_{t-3} \pi^{av}_{t+h}$, imply that SPF forecasts $\mathcal{F}_t \pi^{av}_{t+h}$ and model-based forecasts $E^*_t \pi^{av}_{t+h}$ are nested. That is, they are the same when $\alpha_h = 0$. Indeed, after solving for the expectations components with any assumption regarding rationality or bounded rationality, the solution for expectation terms always have the form $E_t^* \pi_{t+h}^{av} = A_h \mathcal{X}_{t-1} + B_h \xi_t$, where $\mathcal{X}_{t-1}$ is a vector of lagged state variables in state-space form, ξ_t is a vector os contemporaneous shocks, and A_h and B_h are row vectors based on the model parameters. Since $\mathcal{F}_{t-3}\pi_{t+h}^{av}$ already is a lagged state variable, for it is the 3-month lagged value of $\mathcal{F}_t\pi_{t+h+3}^{av}$, the solution for $\mathcal{F}_t\pi_{t+h}^{av}$ must have the form $\mathcal{F}_t\pi_{t+h}^{av} = (1-\alpha_h)(A_h\mathcal{X}_{t-1} + B_h\xi_t) + \alpha_h\mathcal{F}_{t-3}\pi_{t+h}^{av} = (1-\alpha_h) A_h\mathcal{X}_{t-1} + \alpha_h\mathcal{F}_{t-3}\pi_{t+h}^{av} + (1-\alpha_h) B_h\xi_t$. Hence, the linear regression equations for $\mathcal{F}_t\pi_{t+h}^{av}$ and $E_t^*\pi_{t+h}^{av}$ as functions of lagged state variables are nested.

Given the nested models issue, we consider the conditional approach of the Giacomini and White (2006) (GW) test the most appropriate in our case. Even though the usual Diebold and Mariano (1995) (DM) test is not suited for nested models caparisons, we also show its results for robustness checks.

We run pseudo out-of-sample forecasts performance comparisons in two exercises, differing with regard to the type of estimation window. The first one consists of estimating the models with rolling window samples of increasing size, with at least 15 years of mixed-frequency data. That is, we set the beginning of each sample at the same period, and observe monthly (non-seasonally adjusted) headline CPI inflation rates and SPF quarterly forecasts for the 6 forecasting horizons $h \in \{-3, 0, 3, 6, 9, 12\}$. However, the Giacomini and White (2006) test is originally based on forecasts built after estimating models with fixed-size rolling window samples. Therefore, our second exercise uses samples with 15 years of data. In this case, each fixed estimation window has always 180 observations of monthly (non-seasonally adjusted) headline CPI inflation rate,[17] as well as 6×60 observations of quarterly SPF forecasts. Therefore, each fixed window has always a total of $180 + 6 \cdot 60 = 540$ observations. Each increasing-size sample, on the other hand, has at least 540 observations.

In both exercises, we set the samples to start in Januaries and end in Decembers, mimicking an econometrician that reestimates her model once a year, after BLS releases previous December's inflation rate. And so, we use the same estimated parameters throughout each year, before reestimating them in the next January. Since the Philadelphia Fed only took over the SPF in the third quarter of 1990, increasing size samples all begin in January 1991. The first increasing-size sample spans from January 1991 to December 2005, and the last one spans from January 1991 to December 2021. As for the 15-year window samples, the first one spans from January 1991 to

[17]Recall that, in estimating the models, we only observe SPF forecasts and headline (non seasonally adjusted) CPI inflation, and so seasonal adjustments are internally carried out in the model. As mentioned before, this strategy avoids the issue of dealing with vintages of seasonally adjusted CPI inflation in estimation exercises.

December 2005, and the last one spans from January 2007 to December 2021. Both exercises set their testing windows at January 2006 to June 2023.

In each exercise, we estimate 13 parameters, i.e. 7 for the forecasts' laws of motion $\Theta_f \equiv [\alpha_{-3}, \alpha_0, \alpha_3, \alpha_6, \alpha_9, \alpha_{12}, \sigma_{\mathfrak{s}}]$ and 6 for the DGP $\Theta_d \equiv [\rho_{mr}, \rho_{sr}, \sigma_{mr}, \sigma_{sr}, \sigma_{lr}, \sigma_{sea}]$. As previously detailed, models $\text{SF}_{\mathcal{H}}$ impose $\alpha_h = \bar{\alpha}_{\mathcal{H}}$, for all horizons $h \geq H$.

For each model, in both exercises, we start by computing pseudo out-of-sample forecasts for logarithmized quantities using the models' filtered distributions to retrieve (seasonally adjusted) $E_t^* \pi_{t+h}^{av}$ and $E_{t-2}\pi_{t+h}^{av}$, for $h \in \{-3, 0, 3, 6, 9, 12\}$. We design the information set so that filtered distributions provide what econometricians would obtain as seasonally-adjusted forecasts in each period after observing recent available information. That is, at each month $t \in [1, ..., T]$, the available information set contains past realizations of monthly headline (non seasonally adjusted) CPI inflation rates up to month $(t-2)$. And, if month t is the pivot month (second month) of a quarter, the information set also contains current and past aggregate quarterly SPF backcasts/nowcasts/forecasts $\mathcal{F}_t \pi_{t+h}^{av}$, for $h \in \{-3, 0, 3, 6, 9, 12\}$. Since SPF forecasts are only available in quarterly frequency, we use this frequency in our performance tests. Below, we detail how we build quarterly forecasts and their forecast errors.

After retrieving (logarithmized) filtered values of forecasted (logarithmized) average-price rates $E_t^* \pi_{t+h}^{av}$ and $E_{t-2}\pi_{t+h}^{av}$ for each pivot month t, we convert them back to annualized forecast levels $\pi_{t,t+h}^{av^*} = 100\left[\exp\left(4\frac{E_t^*\pi_{t+h}^{av}}{100}\right) - 1\right]$ and $\pi_{t-2,t+h}^{av} = 100\left[\exp\left(4\frac{E_{t-2}\pi_{t+h}^{av}}{100}\right) - 1\right]$.[18] In the effective testing window 2006:Q1 to 2023:Q2, we have 70 backcasts $\pi_{t,t-3}^{av^*}$ and $\pi_{t-2,t-3}^{av}$, 70 nowcasts $\pi_{t,t}^{av^*}$ and $\pi_{t-2,t}^{av}$, and $\left(70 - \frac{h}{3}\right)$ forecasts $\pi_{t,t+h}^{av^*}$ and $\pi_{t-2,t+h}^{av}$ for each future horizon $h \in \{3, 6, 9, 12\}$. Since SPF forecasts are observed as quarterly logarithmized units in the model, annualized SPF forecasts are simply retrieved as $\pi_{t,t+h}^{spf} = 100\left[\exp\left(4\frac{\mathcal{F}_t\pi_{t+h}^{av}}{100}\right) - 1\right]$.

Before computing forecast errors, we need to retrieve realized average-price rates $\pi_{r,t}^{av}$, where we use the subscript r to highlight realized observations. For that, we consider the final vintage of realized seasonally adjusted monthly CPI indices $P_{r,t}^{sa}$, available in July 2023. With those

[18] A slightly more precise approach nonetheless delivers just about the same results as those we show in the paper. After retrieving the models' filtered distributions of $E_t^*\pi_{t+j}^{sa}$ and $E_{t-2}\pi_{t+j}^{sa}$, we set $P_{t,t-7}^{sa^*} = 1$ and $P_{t-2,t-7}^{sa} = 1$. Next, for each j, we sequentially compute $P_{t,t+j}^{sa^*} = P_{t,t+j-1}^{sa^*} \exp\left(E_t^*\pi_{t+j}^{sa}/100\right)$ and $P_{t-2,t+j}^{sa} = P_{t-2,t+j-1}^{sa} \exp\left(E_{t-2}\pi_{t+j}^{sa}/100\right)$. After that, for each SPF horizon h, we obtain forecasted quarterly average prices $P_{t,t+h}^{av^*} = \frac{1}{3}\left(P_{t,t+h+1}^{sa^*} + P_{t,t+h}^{sa^*} + P_{t,t+h-1}^{sa^*}\right)$ and $P_{t-2,t+h}^{av} = \frac{1}{3}\left(P_{t-2,t+h+1}^{sa} + P_{t-2,t+h}^{sa} + P_{t-2,t+h-1}^{sa}\right)$. And then we compute $\pi_{t,t+h}^{av^*} = 100\left[\left(P_{t,t+h}^{av^*}/P_{t,t+h-3}^{av^*}\right)^4 - 1\right]$ and $\pi_{t-2,t+h}^{av} = 100\left[\left(P_{t-2,t+h}^{av}/P_{t-2,t+h-3}^{av}\right)^4 - 1\right]$.

prices, we compute realized average-prices $P^{av}_{r,t} = \frac{1}{3}\left(P^{sa}_{r,t+1} + P^{sa}_{r,t} + P^{sa}_{r,t-1}\right)$ and their quarterly rate $\pi^{av}_{r,t} = 100\left[\left(\frac{P^{av}_{r,t}}{P^{av}_{r,t-3}}\right)^4 - 1\right]$. After that, we compute errors for SPF model-based forecasts: (i) $\xi^{spf}_{t,t+h} = \pi^{spf}_{t,t+h} - \pi^{av}_{r,t+h}$ for SPF forecasts; (ii) $\xi^{av^*}_{t,t+h} = \pi^{av^*}_{t,t+h} - \pi^{av}_{r,t+h}$ for model-based best forecasts; and (iii) $\xi^{av}_{t-2,t+h} = \pi^{av}_{t-2,t+h} - \pi^{av}_{r,t+h}$ for model-based lagged forecasts.

For explanation simplicity, we talk about forecasts built with loglinearized relations $E^*_t\pi^{av}_{t+h} = E_{t-2}\pi^{av}_{t+h} + \mathfrak{s}^{av}_{h,t}$ and $E_{t-2}\pi^{av}_{t+h}$ when meaning $\pi^{av^*}_{t,t+h}$ and $\pi^{av}_{t-2,t+h}$. Notice the estimation samples as well as the testing window were subjected to methodological and stressful events that might have had important temporary and permanent effects on US inflation dynamics and volatility, due to demand, supply and policy changes, such as: (i) the implementation in 1999 of important changes of the 1998 sixth comprehensive CPI revision,[19] which included new housing sample and estimator, computer-assisted data collection for commodities and services sample, shift from area sample rotation to item category rotation using telephone Point-of-Purchase Survey, and redesigned Consumer Expenditure Survey processing system; (ii) the September 11, 2001, attack; (iii) the 2007–2009 Global Financial Crisis, and 2020-2023 COVID-19 pandemics; and (iv) changes in monetary policy due to zero lower bound on nominal interest rates, quantitative easing, negative long-run real interest rates. Despite those methodological and stressful events, we do not exclude any period from the analyses and keep all forecasting errors during the analyses shown below.

For increasing-size sample windows, Tables 3 (models restricting $\alpha_{-3} = 0$) and 4 (unrestricted models) show forecast performance statistics for $\pi^{av^*}_{t,t+h}$ and $\pi^{av}_{t-2,t+h}$ relative to those of SPF. The first column shows SPF Mean Square Errors (MSE), i.e. $mean\left(\xi^{spf}_{t,t+h}\right)^2$, while the remaining columns depict the models' Relative Mean Square Errors (Relative MSE), i.e. $\frac{mean\left(\xi^{av^*}_{t,t+h}\right)^2}{mean\left(\xi^{spf}_{t,t+h}\right)^2}$ and $\frac{mean\left(\xi^{av}_{t-2,t+h}\right)^2}{mean\left(\xi^{spf}_{t,t+h}\right)^2}$. Tables 5 and 6 show the same results for 15–year fixed size sample windows. The tables show p-values from both the Giacomini and White (2006) (GW) and Diebold and Mariano (1995) (DM) tests for predictive ability. Since the GW test is the most appropriate, as compared models as nested, significance stars reflect GW p-values. Ratios smaller than unity means the models' forecasts are better than SPF forecasts. For the GW test, we consider the conditional one. For the DM test, we use Newey-West covariance matrices and sample size correction.[20]

0.56^2

[19] See Greenlees and Mason (1996) for more details.

[20] The lag selection parameter L^* is based on Andrews and Monahan (1992): $L^* = floor\left(4\left(\frac{T}{100}\right)^{\frac{2}{9}}\right)$, where T is the sample size. As for the bandwidth value bm, we use $bm = 1 + L^*$.

Table 3: Forecast Performance - Increasing-Size Sample Windows

Restricted Models with $\alpha_{-3} = 0$

	MSE	Relative MSE for $\pi^{av*}_{t,t+h}$						
h	SPF	RFR	SF$_{-3}$	SF$_0$	SF$_3$	SF$_6$	SF$_9$	SF$_{12}$
-3	0.300	1.000 – –	1.000 – –	1.000 – –	1.000 – –	1.000 – –	1.000 – –	1.000 – –
0	2.408	1.000 – –	1.000 – –	0.557*** p_{GW}=0.003 p_{DM}=0.043	0.565*** p_{GW}=0.010 p_{DM}=0.044	0.566*** p_{GW}=0.005 p_{DM}=0.042	0.565*** p_{GW}=0.005 p_{DM}=0.042	0.567*** p_{GW}=0.004 p_{DM}=0.041
3	7.221	1.000 – –	1.000 – –	0.967 p_{GW}=0.321 p_{DM}=0.237	0.954 p_{GW}=0.862 p_{DM}=0.706	0.974 p_{GW}=0.938 p_{DM}=0.828	0.972 p_{GW}=0.936 p_{DM}=0.817	0.939 p_{GW}=0.805 p_{DM}=0.600
6	8.071	1.000 – –	1.000 – –	1.005 p_{GW}=0.146 p_{DM}=0.690	1.023 p_{GW}=0.397 p_{DM}=0.659	1.070 p_{GW}=0.315 p_{DM}=0.363	1.070 p_{GW}=0.330 p_{DM}=0.364	1.046 p_{GW}=0.512 p_{DM}=0.496
9	8.196	1.000 – –	1.000 – –	1.004 p_{GW}=0.867 p_{DM}=0.725	1.020 p_{GW}=0.543 p_{DM}=0.669	1.058 p_{GW}=0.382 p_{DM}=0.427	1.064 p_{GW}=0.497 p_{DM}=0.399	1.042 p_{GW}=0.445 p_{DM}=0.505
12	8.101	1.000 – –	1.000 – –	0.994 p_{GW}=0.116 p_{DM}=0.459	0.978 p_{GW}=0.121 p_{DM}=0.525	0.978 p_{GW}=0.132 p_{DM}=0.676	0.983 p_{GW}=0.128 p_{DM}=0.725	0.977* p_{GW}=0.093 p_{DM}=0.688

	MSE	Relative MSE for $\pi^{av}_{t-2,t+h}$						
h	SPF	RFR	SF$_{-3}$	SF$_0$	SF$_3$	SF$_6$	SF$_9$	SF$_{12}$
-3	0.300	0.967* p_{GW}=0.066 p_{DM}=0.218	0.967* p_{GW}=0.066 p_{DM}=0.218	0.980 p_{GW}=0.178 p_{DM}=0.794	0.953 p_{GW}=0.714 p_{DM}=0.713	0.941 p_{GW}=0.719 p_{DM}=0.666	0.943 p_{GW}=0.669 p_{DM}=0.681	0.950 p_{GW}=0.654 p_{DM}=0.719
0	2.408	1.050 p_{GW}=0.227 p_{DM}=0.105	1.050 p_{GW}=0.227 p_{DM}=0.105	0.614*** p_{GW}=0.003 p_{DM}=0.034	0.795 p_{GW}=0.125 p_{DM}=0.166	0.912* p_{GW}=0.071 p_{DM}=0.854	0.980* p_{GW}=0.065 p_{DM}=0.847	0.877* p_{GW}=0.099 p_{DM}=0.350
3	7.221	1.044 p_{GW}=0.138 p_{DM}=0.103	1.044 p_{GW}=0.138 p_{DM}=0.103	1.026 p_{GW}=0.379 p_{DM}=0.315	1.003 p_{GW}=0.264 p_{DM}=0.979	0.992 p_{GW}=0.494 p_{DM}=0.942	0.992 p_{GW}=0.452 p_{DM}=0.940	0.998 p_{GW}=0.261 p_{DM}=0.986
6	8.071	1.003 p_{GW}=0.690 p_{DM}=0.714	1.003 p_{GW}=0.690 p_{DM}=0.714	1.003 p_{GW}=0.663 p_{DM}=0.836	0.978 p_{GW}=0.561 p_{DM}=0.773	1.032 p_{GW}=0.415 p_{DM}=0.774	1.032 p_{GW}=0.408 p_{DM}=0.774	1.000 p_{GW}=0.519 p_{DM}=0.998
9	8.196	1.010 p_{GW}=0.492 p_{DM}=0.260	1.010 p_{GW}=0.492 p_{DM}=0.260	1.011 p_{GW}=0.322 p_{DM}=0.284	0.995 p_{GW}=0.391 p_{DM}=0.881	1.035 p_{GW}=0.679 p_{DM}=0.630	1.038 p_{GW}=0.616 p_{DM}=0.612	1.012 p_{GW}=0.904 p_{DM}=0.846
12	8.101	1.019 p_{GW}=0.226 p_{DM}=0.171	1.019 p_{GW}=0.226 p_{DM}=0.171	1.013 p_{GW}=0.291 p_{DM}=0.321	1.034 p_{GW}=0.544 p_{DM}=0.356	1.050 p_{GW}=0.554 p_{DM}=0.375	1.051 p_{GW}=0.558 p_{DM}=0.348	1.023 p_{GW}=0.288 p_{DM}=0.621

Notes: Restricted models with $\alpha_{-3} = 0$. Increasing-Size Sample Windows. First sample: Jan. 1991 to Dec. 2005. Last sample: Jan. 1991 to Dec. 2021. Quarterly testing window: 2006Q1 to 2023Q2. Relative Mean Square Errors (Relative MSE) are $\frac{mean\left(\xi^{av*}_{t,t+h}\right)^2}{mean\left(\xi^{spf}_{t,t+h}\right)^2}$ and $\frac{mean\left(\xi^{av}_{t-2,t+h}\right)^2}{mean\left(\xi^{spf}_{t,t+h}\right)^2}$, and p-values are from both the unconditional Giacomini and White (2006) (GW) and Diebold and Mariano (1995) (DM) tests for predictive ability. Ratios smaller than unity means models‘ forecasts are better than SPF forecasts. Significance notation: 1% (***), 5% (**) and 10% (*) for ratios smaller than unity, and 1% (·), 5% (··) and 10% (·) for ratios larger than unity.

Table 4: Forecast Performance - Increasing-Size Sample Windows

Unrestricted Models

	MSE	Relative MSE for $\pi^{av*}_{t,t+h}$						
h	SPF	RFR	SF-3	SF0	SF3	SF6	SF9	SF12
-3	0.300	1.000 – –	$2.000^{\cdots}$ p_{GW}=0.001 p_{DM}=0.000	1.083 p_{GW}=0.145 p_{DM}=0.027	$1.129^{\cdots}$ p_{GW}=0.008 p_{DM}=0.000	$1.230^{\cdots}$ p_{GW}=0.006 p_{DM}=0.000	$1.230^{\cdots}$ p_{GW}=0.006 p_{DM}=0.000	$1.247^{\cdots}$ p_{GW}=0.006 p_{DM}=0.000
0	2.408	1.000 – –	0.827*** p_{GW}=0.001 p_{DM}=0.008	0.548*** p_{GW}=0.005 p_{DM}=0.045	0.551** p_{GW}=0.015 p_{DM}=0.049	0.534*** p_{GW}=0.010 p_{DM}=0.053	0.533*** p_{GW}=0.010 p_{DM}=0.053	0.543*** p_{GW}=0.010 p_{DM}=0.050
3	7.221	1.000 – –	0.991 p_{GW}=0.453 p_{DM}=0.362	0.966 p_{GW}=0.324 p_{DM}=0.236	0.941 p_{GW}=0.831 p_{DM}=0.628	0.989 p_{GW}=0.912 p_{DM}=0.927	0.987 p_{GW}=0.919 p_{DM}=0.915	0.948 p_{GW}=0.868 p_{DM}=0.674
6	8.071	1.000 – –	1.001 p_{GW}=0.628 p_{DM}=0.839	1.005 p_{GW}=0.153 p_{DM}=0.681	1.023 p_{GW}=0.428 p_{DM}=0.665	1.085 p_{GW}=0.291 p_{DM}=0.317	1.085 p_{GW}=0.300 p_{DM}=0.316	1.060 p_{GW}=0.450 p_{DM}=0.419
9	8.196	1.000 – –	1.001 p_{GW}=0.955 p_{DM}=0.893	1.005 p_{GW}=0.857 p_{DM}=0.707	1.021 p_{GW}=0.511 p_{DM}=0.674	1.070 p_{GW}=0.337 p_{DM}=0.387	1.076 p_{GW}=0.453 p_{DM}=0.365	1.054 p_{GW}=0.361 p_{DM}=0.439
12	8.101	1.000 – –	0.997 p_{GW}=0.106 p_{DM}=0.298	0.994 p_{GW}=0.113 p_{DM}=0.460	0.979 p_{GW}=0.112 p_{DM}=0.591	0.979 p_{GW}=0.136 p_{DM}=0.713	0.984 p_{GW}=0.132 p_{DM}=0.762	0.977* p_{GW}=0.096 p_{DM}=0.725

	MSE	Relative MSE for $\pi^{av}_{t-2,t+h}$						
h	SPF	RFR	SF-3	SF0	SF3	SF6	SF9	SF12
-3	0.300	0.967* p_{GW}=0.066 p_{DM}=0.218	$1.887^{\cdots}$ p_{GW}=0.002 p_{DM}=0.000	1.059 p_{GW}=0.297 p_{DM}=0.450	1.007 p_{GW}=0.932 p_{DM}=0.960	1.037 p_{GW}=0.857 p_{DM}=0.826	1.041 p_{GW}=0.790 p_{DM}=0.808	1.043 p_{GW}=0.777 p_{DM}=0.794
0	2.408	1.050 p_{GW}=0.227 p_{DM}=0.105	0.874*** p_{GW}=0.002 p_{DM}=0.003	0.604*** p_{GW}=0.004 p_{DM}=0.036	0.780 p_{GW}=0.153 p_{DM}=0.163	0.962* p_{GW}=0.057 p_{DM}=0.722	0.960* p_{GW}=0.059 p_{DM}=0.718	0.872 p_{GW}=0.120 p_{DM}=0.377
3	7.221	1.044 p_{GW}=0.138 p_{DM}=0.103	1.024 p_{GW}=0.167 p_{DM}=0.070	1.025 p_{GW}=0.420 p_{DM}=0.347	1.001 p_{GW}=0.298 p_{DM}=0.996	0.995 p_{GW}=0.546 p_{DM}=0.966	0.994 p_{GW}=0.505 p_{DM}=0.962	1.001 p_{GW}=0.300 p_{DM}=0.996
6	8.071	1.003 p_{GW}=0.690 p_{DM}=0.714	1.002 p_{GW}=0.297 p_{DM}=0.847	1.003 p_{GW}=0.711 p_{DM}=0.832	0.982 p_{GW}=0.464 p_{DM}=0.827	1.043 p_{GW}=0.425 p_{DM}=0.717	1.044 p_{GW}=0.418 p_{DM}=0.718	1.009 p_{GW}=0.512 p_{DM}=0.926
9	8.196	1.010 p_{GW}=0.492 p_{DM}=0.260	1.010 p_{GW}=0.333 p_{DM}=0.225	1.011 p_{GW}=0.300 p_{DM}=0.264	0.995 p_{GW}=0.312 p_{DM}=0.907	1.043 p_{GW}=0.709 p_{DM}=0.595	1.046 p_{GW}=0.649 p_{DM}=0.578	1.020 p_{GW}=0.889 p_{DM}=0.772
12	8.101	1.019 p_{GW}=0.226 p_{DM}=0.171	1.019 p_{GW}=0.156 p_{DM}=0.161	1.014 p_{GW}=0.291 p_{DM}=0.312	1.017 p_{GW}=0.593 p_{DM}=0.521	1.056 p_{GW}=0.515 p_{DM}=0.366	1.058 p_{GW}=0.523 p_{DM}=0.341	1.029 p_{GW}=0.248 p_{DM}=0.573

Notes: Unrestricted models. Increasing-Size Sample Windows. First sample: Jan. 1991 to Dec. 2005. Last sample: Jan. 1991 to Dec. 2021. Quarterly testing window: 2006Q1 to 2023Q2. Relative Mean Square Errors (Relative MSE) are $\frac{mean\left(\xi^{av^*}_{t,t+h}\right)^2}{mean\left(\xi^{spf}_{t,t+h}\right)^2}$ and $\frac{mean\left(\xi^{av}_{t-2,t+h}\right)^2}{mean\left(\xi^{spf}_{t,t+h}\right)^2}$, and p-values are from both the unconditional Giacomini and White (2006) (GW) and Diebold and Mariano (1995) (DM) tests for predictive ability. Ratios smaller than unity means models' forecasts are better than SPF forecasts. Significance notation: 1% (***), 5% (**) and 10% (*) for ratios smaller than unity, and 1% (···), 5% (··) and 10% (·) for ratios larger than unity.

Table 5: Forecast Performance - 15-Year Fixed-Size Sample Windows

Restricted Models with $\alpha_{-3} = 0$

	MSE	Relative MSE for $\pi^{av*}_{t,t+h}$						
h	SPF	RFR	SF-3	SF0	SF3	SF6	SF9	SF12
-3	0.300	1.000 – –	1.000 – –	1.000 – –	1.000 – –	1.000 – –	1.000 – –	1.000 – –
0	2.408	1.000 – –	1.000 – –	0.575*** p_{GW}=0.002 p_{DM}=0.041	0.569*** p_{GW}=0.009 p_{DM}=0.043	0.592*** p_{GW}=0.006 p_{DM}=0.039	0.572*** p_{GW}=0.005 p_{DM}=0.043	0.576*** p_{GW}=0.005 p_{DM}=0.042
3	7.221	1.000 – –	1.000 – –	0.971 p_{GW}=0.337 p_{DM}=0.235	0.930 p_{GW}=0.756 p_{DM}=0.556	0.951 p_{GW}=0.844 p_{DM}=0.682	0.955 p_{GW}=0.907 p_{DM}=0.706	0.942 p_{GW}=0.845 p_{DM}=0.629
6	8.071	1.000 – –	1.000 – –	1.005 p_{GW}=0.144 p_{DM}=0.667	1.013 p_{GW}=0.531 p_{DM}=0.788	1.062 p_{GW}=0.528 p_{DM}=0.416	1.103 p_{GW}=0.386 p_{DM}=0.288	1.084 p_{GW}=0.514 p_{DM}=0.353
9	8.196	1.000 – –	1.000 – –	1.004 p_{GW}=0.856 p_{DM}=0.716	1.012 p_{GW}=0.505 p_{DM}=0.799	1.047 p_{GW}=0.169 p_{DM}=0.504	1.066 p_{GW}=0.397 p_{DM}=0.403	1.042 p_{GW}=0.340 p_{DM}=0.516
12	8.101	1.000 – –	1.000 – –	0.995 p_{GW}=0.113 p_{DM}=0.520	0.987 p_{GW}=0.119 p_{DM}=0.734	1.054 p_{GW}=0.675 p_{DM}=0.365	1.058 p_{GW}=0.560 p_{DM}=0.264	1.063 p_{GW}=0.562 p_{DM}=0.288

	MSE	Relative MSE for $\pi^{av}_{t-2,t+h}$						
h	SPF	RFR	SF-3	SF0	SF3	SF6	SF9	SF12
-3	0.300	0.960* p_{GW}=0.059 p_{DM}=0.184	0.960* p_{GW}=0.059 p_{DM}=0.184	0.977 p_{GW}=0.181 p_{DM}=0.751	0.944 p_{GW}=0.781 p_{DM}=0.635	0.926 p_{GW}=0.711 p_{DM}=0.554	0.941 p_{GW}=0.806 p_{DM}=0.655	0.944 p_{GW}=0.812 p_{DM}=0.673
0	2.408	1.050 p_{GW}=0.183 p_{DM}=0.086	1.050 p_{GW}=0.183 p_{DM}=0.086	0.630*** p_{GW}=0.002 p_{DM}=0.032	0.763* p_{GW}=0.094 p_{DM}=0.139	0.925* p_{GW}=0.100 p_{DM}=0.628	1.002 p_{GW}=0.113 p_{DM}=0.990	0.914* p_{GW}=0.091 p_{DM}=0.587
3	7.221	1.051$^{\cdot}$ p_{GW}=0.094 p_{DM}=0.075	1.051$^{\cdot}$ p_{GW}=0.094 p_{DM}=0.075	1.033 p_{GW}=0.297 p_{DM}=0.111	0.992 p_{GW}=0.174 p_{DM}=0.945	1.018 p_{GW}=0.250 p_{DM}=0.862	1.003 p_{GW}=0.585 p_{DM}=0.982	1.017 p_{GW}=0.370 p_{DM}=0.873
6	8.071	1.009 p_{GW}=0.790 p_{DM}=0.511	1.009 p_{GW}=0.790 p_{DM}=0.511	1.011 p_{GW}=0.517 p_{DM}=0.376	0.979 p_{GW}=0.409 p_{DM}=0.744	0.984 p_{GW}=0.800 p_{DM}=0.839	1.033 p_{GW}=0.367 p_{DM}=0.759	1.002 p_{GW}=0.649 p_{DM}=0.984
9	8.196	1.014 p_{GW}=0.499 p_{DM}=0.277	1.014 p_{GW}=0.499 p_{DM}=0.277	1.017 p_{GW}=0.275 p_{DM}=0.217	1.001$^{\cdot}$ p_{GW}=0.061 p_{DM}=0.977	0.992 p_{GW}=0.955 p_{DM}=0.878	1.030 p_{GW}=0.477 p_{DM}=0.685	1.007 p_{GW}=0.778 p_{DM}=0.902
12	8.101	1.020 p_{GW}=0.215 p_{DM}=0.170	1.020 p_{GW}=0.215 p_{DM}=0.170	1.019 p_{GW}=0.241 p_{DM}=0.232	1.023 p_{GW}=0.232 p_{DM}=0.191	1.021 p_{GW}=0.714 p_{DM}=0.658	1.024 p_{GW}=0.715 p_{DM}=0.601	1.015 p_{GW}=0.499 p_{DM}=0.718

Notes: Restricted models with $\alpha_{-3} = 0$. 15-Year Fixed-Size Sample Windows. First sample: Jan. 1991 to Dec. 2005. Last sample: Jan. 2007 to Dec. 2021. Quarterly testing window: 2006Q1 to 2023Q2. Relative Mean Square Errors (Relative MSE) are $\frac{mean\left(\xi^{av*}_{t,t+h}\right)^2}{mean\left(\xi^{spf}_{t,t+h}\right)^2}$ and $\frac{mean\left(\xi^{av}_{t-2,t+h}\right)^2}{mean\left(\xi^{spf}_{t,t+h}\right)^2}$, and p-values are from both the unconditional Giacomini and White (2006) (GW) and Diebold and Mariano (1995) (DM) tests for predictive ability. Ratios smaller than unity means models' forecasts are better than SPF forecasts. Significance notation: 1% (***), 5% (**) and 10% (*) for ratios smaller than unity, and 1% (·), 5% (··) and 10% (·) for ratios bigger than unity.

Table 6: Forecast Performance - 15-Year Fixed-Size Sample Windows

Unrestricted Models

	MSE	Relative MSE for $\pi^{av*}_{t,t+h}$						
h	SPF	RFR	SF$_{-3}$	SF$_0$	SF$_3$	SF$_6$	SF$_9$	SF$_{12}$
-3	0.300	1.000 – –	2.180$^{\cdot\cdot\cdot}$ p_{GW}=0.001 p_{DM}=0.000	1.183$^{\cdot\cdot}$ p_{GW}=0.028 p_{DM}=0.003	1.160$^{\cdot\cdot\cdot}$ p_{GW}=0.006 p_{DM}=0.000	1.255$^{\cdot\cdot\cdot}$ p_{GW}=0.003 p_{DM}=0.000	1.227$^{\cdot\cdot\cdot}$ p_{GW}=0.006 p_{DM}=0.000	1.261$^{\cdot\cdot\cdot}$ p_{GW}=0.004 p_{DM}=0.000
0	2.408	1.000 – –	0.801*** p_{GW}=0.000 p_{DM}=0.016	0.572*** p_{GW}=0.002 p_{DM}=0.043	0.563** p_{GW}=0.016 p_{DM}=0.050	0.578** p_{GW}=0.013 p_{DM}=0.048	0.542*** p_{GW}=0.010 p_{DM}=0.055	0.558** p_{GW}=0.012 p_{DM}=0.052
3	7.221	1.000 – –	0.985 p_{GW}=0.154 p_{DM}=0.245	0.971 p_{GW}=0.339 p_{DM}=0.238	0.951 p_{GW}=0.832 p_{DM}=0.700	0.958 p_{GW}=0.873 p_{DM}=0.741	0.968 p_{GW}=0.940 p_{DM}=0.799	0.952 p_{GW}=0.897 p_{DM}=0.705
6	8.071	1.000 – –	0.998 p_{GW}=0.272 p_{DM}=0.758	1.006 p_{GW}=0.156 p_{DM}=0.629	1.019 p_{GW}=0.443 p_{DM}=0.713	1.077 p_{GW}=0.461 p_{DM}=0.357	1.123 p_{GW}=0.324 p_{DM}=0.245	1.102 p_{GW}=0.440 p_{DM}=0.303
9	8.196	1.000 – –	0.999 p_{GW}=0.862 p_{DM}=0.884	1.005 p_{GW}=0.835 p_{DM}=0.682	1.016 p_{GW}=0.481 p_{DM}=0.744	1.059 p_{GW}=0.142 p_{DM}=0.441	1.079 p_{GW}=0.360 p_{DM}=0.361	1.052 p_{GW}=0.295 p_{DM}=0.462
12	8.101	1.000 – –	0.995 p_{GW}=0.146 p_{DM}=0.262	0.995 p_{GW}=0.112 p_{DM}=0.519	0.984 p_{GW}=0.120 p_{DM}=0.678	1.064 p_{GW}=0.643 p_{DM}=0.328	1.068 p_{GW}=0.530 p_{DM}=0.233	1.077 p_{GW}=0.525 p_{DM}=0.240

	MSE	Relative MSE for $\pi^{av}_{t-2,t+h}$						
h	SPF	RFR	SF$_{-3}$	SF$_0$	SF$_3$	SF$_6$	SF$_9$	SF$_{12}$
-3	0.300	0.960* p_{GW}=0.059 p_{DM}=0.184	2.068$^{\cdot\cdot\cdot}$ p_{GW}=0.001 p_{DM}=0.001	1.178$^{\cdot\cdot}$ p_{GW}=0.034 p_{DM}=0.033	1.031 p_{GW}=0.912 p_{DM}=0.824	1.014 p_{GW}=0.997 p_{DM}=0.921	1.041 p_{GW}=0.979 p_{DM}=0.797	1.043 p_{GW}=0.968 p_{DM}=0.786
0	2.408	1.050 p_{GW}=0.183 p_{DM}=0.086	0.845*** p_{GW}=0.000 p_{DM}=0.015	0.621*** p_{GW}=0.002 p_{DM}=0.034	0.763 p_{GW}=0.112 p_{DM}=0.149	0.924 p_{GW}=0.113 p_{DM}=0.647	0.960* p_{GW}=0.059 p_{DM}=0.895	0.916 p_{GW}=0.108 p_{DM}=0.624
3	7.221	1.051$^{\cdot}$ p_{GW}=0.094 p_{DM}=0.075	1.015 p_{GW}=0.335 p_{DM}=0.298	1.021 p_{GW}=0.139 p_{DM}=0.422	0.999 p_{GW}=0.162 p_{DM}=0.996	1.023 p_{GW}=0.266 p_{DM}=0.834	0.994 p_{GW}=0.505 p_{DM}=0.946	1.022 p_{GW}=0.390 p_{DM}=0.846
6	8.071	1.009 p_{GW}=0.790 p_{DM}=0.511	0.998 p_{GW}=0.230 p_{DM}=0.853	1.002 p_{GW}=0.971 p_{DM}=0.878	0.976 p_{GW}=0.549 p_{DM}=0.725	0.989 p_{GW}=0.822 p_{DM}=0.896	1.044 p_{GW}=0.418 p_{DM}=0.696	1.010 p_{GW}=0.644 p_{DM}=0.918
9	8.196	1.014 p_{GW}=0.499 p_{DM}=0.277	1.014 p_{GW}=0.367 p_{DM}=0.248	1.017 p_{GW}=0.262 p_{DM}=0.214	1.001 p_{GW}=0.167 p_{DM}=0.968	0.995 p_{GW}=0.995 p_{DM}=0.932	1.046 p_{GW}=0.649 p_{DM}=0.636	1.013 p_{GW}=0.831 p_{DM}=0.837
12	8.101	1.020 p_{GW}=0.215 p_{DM}=0.170	1.023 p_{GW}=0.195 p_{DM}=0.150	1.020 p_{GW}=0.213 p_{DM}=0.208	1.041 p_{GW}=0.242 p_{DM}=0.215	1.024 p_{GW}=0.605 p_{DM}=0.638	1.058 p_{GW}=0.523 p_{DM}=0.560	1.020 p_{GW}=0.428 p_{DM}=0.672

Notes: Unrestricted models. 15-Year Fixed-Size Sample Windows. First sample: Jan. 1991 to Dec. 2005. Last sample: Jan. 2007 to Dec. 2021. Quarterly testing window: 2006Q1 to 2023Q2. Relative Mean Square Errors (Relative MSE) are $\frac{mean\left(\xi^{av^*}_{t,t+h}\right)^2}{mean\left(\xi^{spf}_{t,t+h}\right)^2}$ and $\frac{mean\left(\xi^{av}_{t-2,t+h}\right)^2}{mean\left(\xi^{spf}_{t,t+h}\right)^2}$, and p-values are from both the unconditional Giacomini and White (2006) (GW) and Diebold and Mariano (1995) (DM) tests for predictive ability. Ratios smaller than unity means models' forecasts are better than SPF forecasts. Significance notation: 1% (***), 5% (**) and 10% (*) for ratios smaller than unity, and 1% (·), 5% (··) and 10% (·) for ratios larger than unity.

We draw four important lessons from the exercises: (i) nowcasts ($h = 0$) performances, i.e. based on $E_t^* \pi_t^{av} = \left(E_{t-2}\pi_t^{av} + \mathfrak{s}_{0,t}^{av}\right)$, are strongly and significantly better than those from SPF; (ii) nowcasts's MSE's built with $E_{t-2}\pi_t^{av}$ are far from being as efficient as those obtained with $E_t^* \pi_t^{av}$; (iii) for backcasts ($h = -3$), SPF dominates the model's forecasts $E_t^* \pi_{t-3}^{av}$ in unrestricted models and are just as efficient (by construction) in restricted models; and (iv) for longer horizons ($h > 0$), the model's forecasts $E_t^* \pi_{t+h}^{av}$ are at par with SPF survey.

As for the first lesson, nowcasts's MSE's (built with $E_t^* \pi_t^{av}$) are about 53%-57% of those obtained from SPF nowcasts. This outcome is important, for we do not add any extra and intra-quarter information, other than monthly nonseasonally adjusted CPI inflation and quarterly SPF forecasts. For comparison, Knotek II and Zaman (2017) find a similar nowcast Relative MSE in a monthly-frequency model, of about $\frac{1}{1.98} = 51\%$,[21] only after including a plethora of external higher-frequency information, meant to match the information set available to SPF responders. In addition to the monthly CPI inflation, the authors extract information from daily oil prices, weekly gasoline prices, and the history of monthly Personal Consumption Expenditure (PCE) rates. Here, we not do not include external information other than that from past non-seasonally adjusted CPI inflation and current SPF forecasts.

As for the second lesson, i.e. regarding the finding that $E_{t-2}\pi_t^{av}$ are far from being as efficient as those obtained with $E_t^* \pi_t^{av} = \left(E_{t-2}\pi_t^{av} + \mathfrak{s}_{0,t}^{av}\right)$, it confirms our assumption that the latent component $\mathfrak{s}_{0,t}^{av}$, retrieved by Kalman filtering, does convey additional soft and intra-quarter information and contributes for forecast improvements. Since we obtain similar nowcast Relative MSE's as those obtained by Knotek II and Zaman (2017) using external data, it suggests the extra external higher-frequency information used by the authors is actually already imbedded into the survey forecasts, and removing the effects of nowcast rigidity is enough for unveiling this purer information.

As for the third and fourth lessons, it implies that removing all forecast rigidity does not always allows for improved forecasts. In particular, our results strongly suggest this approach is recommended for nowcasts, but is not necessarily advisable for the remaining horizons.

[21] See third row of Table 7 in Knotek II and Zaman (2017).

5 Resetting Forecast Dominance

As shown in Section 4, Resetting Nowcasts strongly dominate SPF Average Nowcasts for SPF, but Resetting Forecasts are only just as good for longer horizons. Therefore, it begs the question, *which are the conditions for Resetting Forecasts to dominate Average Forecasts?*

In this section, for simplicity, we answer this question by considering a model with noisy-dispersed information. A more general hybrid formulation with noisy-dispersed and sticky information (e.g. Andrade and Le Bihan (2013) and Areosa, Areosa, and Carrasco (2020)) would only add complexity without changing much the main lessons. For proof of concept purposes, we consider the quarterly frequency and assume a simple data generating process (DGP) for the average price rate.

5.1 Noisy-Dispersed Forecasts

We slightly depart from Coibion and Gorodnichenko (2015) by extending the model to allow for disagreement and horizon-specific parameters. Assume each respondent $i \in [0, 1]$ initially builds raw forecasts $E^{*}_{i,q}\pi^{av}_{q+\mathfrak{h}}$, for each quarterly horizon $\mathfrak{h} \in \{-1, 0, 1, 2, 3, 4\}$. Being subject to noisy information, her initial raw forecast satisfies $E^{*}_{i,q}\pi^{av}_{q+\mathfrak{h}} = \pi^{av}_{q+\mathfrak{h}} + \upsilon_{i,\mathfrak{h},q+\mathfrak{h}}$, where $\upsilon_{i,\mathfrak{h},q+\mathfrak{h}} \sim N\left(0, \sigma^2_{\upsilon,\mathfrak{h}}\right)$ is the individual forecast error for horizon $\mathfrak{h}$. Notice the variance $\sigma^2_{\upsilon,\mathfrak{h}}$ might be horizon-specific.

Unbeknown to each individual forecaster, the forecast error is comprised of a common public noise $\eta_{\mathfrak{h},q+\mathfrak{h}} \sim N\left(0, \sigma^2_{\eta,\mathfrak{h}}\right)$ and a private component $\delta_{i,\mathfrak{h},q+\mathfrak{h}} \sim N\left(0, \sigma^2_{\delta,\mathfrak{h}}\right)$, i.e. $\upsilon_{i,\mathfrak{h},q+\mathfrak{h}} \equiv \left(\eta_{\mathfrak{h},q+\mathfrak{h}} + \delta_{i,\mathfrak{h},q+\mathfrak{h}}\right)$, where $\delta_{i,\mathfrak{h},q+\mathfrak{h}}$ captures dispersion across all individuals, i.e. $\int_0^1 \delta_{i,\mathfrak{h},q+\mathfrak{h}} di = 0$. It implies $\sigma^2_{\upsilon,\mathfrak{h}} \equiv \left(\sigma^2_{\eta,\mathfrak{h}} + \sigma^2_{\delta,\mathfrak{h}}\right)$ and $\int_0^1 \upsilon_{i,\mathfrak{h},q+\mathfrak{h}} di = \eta_{\mathfrak{h},q+\mathfrak{h}}$.

Under certain conditions, Direct Multistep (DMS) models – or direct forecasts – outperform Iterated Multistep (IMS) models in forecasting, and might be robust to model misspecification (e.g. Marcellino, Stock, and Watson (2006) and McCracken and McGillicuddy (2018), among others). Since the DMS models' forecast errors are horizon specific, no iteration is required for producing forecasts. In particular, McCracken and McGillicuddy (2018) find evidence that DMS models are better for forecasting nominal variables such as prices, wages and money.

Therefore, forecasters would have incentives to use DMS models when producing their initial raw forecasts $E^{*}_{i,q}\pi^{av}_{q+\mathfrak{h}}$, retrieved after estimating equations like $\pi^{av}_{q+\mathfrak{h}} = \left(\rho_{\mathfrak{h}}\right)^{\mathfrak{h}+1} \pi^{av}_{q-1} + \xi_{\mathfrak{h},q+\mathfrak{h}}$, where $\left|\rho_{\mathfrak{h}}\right| < 1$ and $\xi_{\mathfrak{h},q+\mathfrak{h}} \sim N\left(0, \sigma^2_{\xi,\mathfrak{h}}\right)$ for each horizon. Direct forecasting is equivalent to assuming horizon-specific DGP processes for inflation, each one aimed at producing recursive forecasts for each specific horizon $\mathfrak{h}$: $\pi_q^{av} = \rho_{\mathfrak{h}} \pi_{q-1}^{av} + \varepsilon_{\mathfrak{h},q}$, where $\varepsilon_{\mathfrak{h},q} \sim N\left(0, \sigma_{\mathfrak{h}}^2\right)$. Note that, no matter the quarterly forecasting horizon $\mathfrak{h}$ and values for parameters for $\rho_{\mathfrak{h}}$, $\sigma_{\varepsilon,\mathfrak{h}}^2$ and $\sigma_{\xi,\mathfrak{h}}^2$, the implied ergodic distribution for π_q^{av} must be the same. That is, if $\bar{\sigma}^2 \equiv var\left(\pi_q^{av}\right)$ is its ergodic variance, the horizon-specific parameters must satisfy $\bar{\sigma}^2 = \frac{\sigma_{\mathfrak{h}}^2}{\left(1-\left(\rho_{\mathfrak{h}}\right)^2\right)} = \frac{\sigma_{\xi,\mathfrak{h}}^2}{\left(1-\left(\rho_{\mathfrak{h}}\right)^{2(\mathfrak{h}+1)}\right)}$.

Each forecaster is aware of its signal $E_{i,q}^* \pi_{q+\mathfrak{h}}^{av} = \pi_{q+\mathfrak{h}}^{av} + \upsilon_{i,\mathfrak{h},q+\mathfrak{h}}$ and state $\pi_q^{av} = \rho_{\mathfrak{h}} \pi_{q-1}^{av} + \varepsilon_{\mathfrak{h},q}$ equations. In addition, at each quarter q, she observes $E_{i,q}^* \pi_{q+\mathfrak{h}}^{av}$ and past values of realized inflation π_{q-k}^{av}, for $k = \{1, 2, ...\}$. Using Kalman filtering, she can improve[22] her initial raw forecast $E_{i,q}^* \pi_{q+\mathfrak{h}}^{av}$ into $\mathcal{F}_{i,q} \pi_{q+\mathfrak{h}}^{av} \equiv E\left(\pi_{q+\mathfrak{h}}^{av} | E_{i,q}^* \pi_{q+\mathfrak{h}}^{av}, \left\{\pi_{q-\tau}^{av}\right\}_{\tau \geq 1}\right)$, where superscript $(^*)$ stands for individual improved forecasts. Kalman recursion delivers:

$$\mathcal{F}_{i,q} \pi_{q+\mathfrak{h}}^{av} = \left(1 - \gamma_{\mathfrak{h}}\right) \mathcal{F}_{i,q-1} \pi_{q+\mathfrak{h}}^{av} + \gamma_{\mathfrak{h}} E_{i,q}^* \pi_{q+\mathfrak{h}}^{av} \tag{10}$$

where $\gamma_{\mathfrak{h}} = \frac{\kappa_{\mathfrak{h}} \bar{\sigma}^2}{\kappa_{\mathfrak{h}} \bar{\sigma}^2 + \sigma_{\upsilon,\mathfrak{h}}^2}$ is the horizon-specific Kalman gain, the inertia-based adjustment factor[23] is $\kappa_{\mathfrak{h}} = \frac{\left(1-\left(\rho_{\mathfrak{h}}\right)^2\right)}{2} \left[\left(1 - \frac{\sigma_{\upsilon,\mathfrak{h}}^2}{\bar{\sigma}^2}\right) + \sqrt{\left(1 - \frac{\sigma_{\upsilon,\mathfrak{h}}^2}{\bar{\sigma}^2}\right)^2 + \frac{4}{\left(1-\left(\rho_{\mathfrak{h}}\right)^2\right)} \frac{\sigma_{\upsilon,\mathfrak{h}}^2}{\bar{\sigma}^2}}\right]$, and $\bar{\sigma}^2 = \frac{\sigma_{\mathfrak{h}}^2}{\left(1-\left(\rho_{\mathfrak{h}}\right)^2\right)}$ is the unconditional variance. Note the reasons leading to horizon-specific Kalman gains $\gamma_{\mathfrak{h}}$ are direct forecasting and horizon-specific error variances.

In turn, the Average Forecast $\mathcal{F}_q \pi_{q+\mathfrak{h}}^{av} \equiv \int_0^1 \mathcal{F}_{i,q} \pi_{q+\mathfrak{h}}^{av} di$ evolves according to

$$\mathcal{F}_q \pi_{q+\mathfrak{h}}^{av} = \left(1 - \gamma_{\mathfrak{h}}\right) \mathcal{F}_{q-1} \pi_{q+\mathfrak{h}}^{av} + \gamma_{\mathfrak{h}} E_q^* \pi_{q+\mathfrak{h}}^{av} \tag{11}$$

where $E_q^* \pi_{q+\mathfrak{h}}^{av} = \int_0^1 E_{i,q}^* \pi_{q+\mathfrak{h}}^{av} di = \pi_{q+\mathfrak{h}}^{av} + \eta_{\mathfrak{h},q+\mathfrak{h}}$ is the Resetting Forecast, not observed by any individual forecaster when providing SPF with $\mathcal{F}_{i,q} \pi_{q+\mathfrak{h}}^{av}$.

Therefore, as shown in Andrade and Le Bihan (2013) and Coibion and Gorodnichenko (2015), the forecast rigidity parameters defined in Section 2.2.3 have a one-to-one mapping into those Kalman gains, i.e. $\alpha_{\mathfrak{h}} = \left(1 - \gamma_{\mathfrak{h}}\right)$.

[22] Given her initial raw forecast $E_{i,q}^* \pi_{q+\mathfrak{h}}^{av} = \pi_{q+\mathfrak{h}}^{av} + \upsilon_{i,\mathfrak{h},q+\mathfrak{h}}$, Kalman filtering leading to $\mathcal{F}_{i,q}^* \pi_{q+\mathfrak{h}}^{av}$ always minimizes the variance of her own forecast errors.

[23] As usual, $\kappa_{\mathfrak{h}} = 1$ if $\rho_{\mathfrak{h}} = 0$.

5.2 Forecast Dominance

Kalman recursion applied to this model implies $\mathcal{F}_{i,q}\pi^{av}_{q+1+\mathfrak{h}} = \rho_{\mathfrak{h}}\mathcal{F}_{i,q}\pi^{av}_{q+\mathfrak{h}}$ and $\mathcal{F}_{q}\pi^{av}_{q+1+\mathfrak{h}} = \rho_{\mathfrak{h}}\mathcal{F}_{q}\pi^{av}_{q+\mathfrak{h}}$. Therefore, using (10) and (11), the Individual Forecast error $\xi_{i,q,\mathfrak{h}} \equiv \mathcal{F}_{i,q}\pi^{av}_{q+\mathfrak{h}} - \pi^{av}_{q+\mathfrak{h}}$, Average Forecast error $\xi_{q,\mathfrak{h}} \equiv \int_0^1 \xi_{i,q,\mathfrak{h}} di = \mathcal{F}_{q}\pi^{av}_{q+\mathfrak{h}} - \pi^{av}_{q+\mathfrak{h}}$, and Resetting Forecast error $\xi^*_{q,\mathfrak{h}} \equiv E^*_q\pi^{av}_{q+\mathfrak{h}} - \pi^{av}_{q+\mathfrak{h}}$ satisfy (see Appendix D):

$$\begin{aligned}
\xi_{i,q,\mathfrak{h}} &= \left(1-\gamma_{\mathfrak{h}}\right)\rho_{\mathfrak{h}}\xi_{i,q-1,\mathfrak{h}} - \left(1-\gamma_{\mathfrak{h}}\right)\varepsilon_{\mathfrak{h},q+\mathfrak{h}} + \gamma_{\mathfrak{h}}\upsilon_{i,\mathfrak{h},q+\mathfrak{h}} \\
\xi_{q,\mathfrak{h}} &= \left(1-\gamma_{\mathfrak{h}}\right)\rho_{\mathfrak{h}}\xi_{q-1,\mathfrak{h}} - \left(1-\gamma_{\mathfrak{h}}\right)\varepsilon_{\mathfrak{h},q+\mathfrak{h}} + \gamma_{\mathfrak{h}}\eta_{\mathfrak{h},q+\mathfrak{h}} \\
\xi^*_{q,\mathfrak{h}} &= \eta_{\mathfrak{h},q+\mathfrak{h}}
\end{aligned}$$

Therefore, their unconditional variances $\vartheta_{i,\mathfrak{h}} \equiv var\left(\xi_{i,q,\mathfrak{h}}\right)$, $\vartheta_{\mathfrak{h}} \equiv var\left(\xi_{q,\mathfrak{h}}\right)$, and $\vartheta^*_{\mathfrak{h}} \equiv var\left(\xi^*_{q,\mathfrak{h}}\right)$ are:

$$\vartheta_{i,\mathfrak{h}} = \frac{\left(1-\gamma_{\mathfrak{h}}\right)^2\sigma^2_{\mathfrak{h}} + \left(\gamma_{\mathfrak{h}}\right)^2\sigma^2_{\upsilon,\mathfrak{h}}}{1-\left(1-\gamma_{\mathfrak{h}}\right)^2\rho^2_{\mathfrak{h}}} \quad ; \; \vartheta_{\mathfrak{h}} = \frac{\left(1-\gamma_{\mathfrak{h}}\right)^2\sigma^2_{\mathfrak{h}} + \left(\gamma_{\mathfrak{h}}\right)^2\sigma^2_{\eta,\mathfrak{h}}}{1-\left(1-\gamma_{\mathfrak{h}}\right)^2\rho^2_{\mathfrak{h}}} \quad ; \; \vartheta^*_{\mathfrak{h}} = \sigma^2_{\eta,\mathfrak{h}} \tag{12}$$

where again $\upsilon_{i,\mathfrak{h},q+\mathfrak{h}} \sim N\left(0,\sigma^2_{\upsilon,\mathfrak{h}}\right)$, $\eta_{\mathfrak{h},q+\mathfrak{h}} \sim N\left(0,\sigma^2_{\eta,\mathfrak{h}}\right)$, $\upsilon_{i,\mathfrak{h},q+\mathfrak{h}} \equiv \left(\eta_{\mathfrak{h},q+\mathfrak{h}} + \delta_{i,\mathfrak{h},q+\mathfrak{h}}\right)$ and $\sigma^2_{\upsilon,\mathfrak{h}} \equiv \left(\sigma^2_{\eta,\mathfrak{h}} + \sigma^2_{\delta,\mathfrak{h}}\right)$.

It is easy to verify that $\vartheta_{i,\mathfrak{h}} \geq \vartheta_{\mathfrak{h}}$. That is, $\vartheta_{i,\mathfrak{h}}$ also accounts for the extra effect of disagreement on top of the variance $\vartheta_{\mathfrak{h}}$ of the Average Forecast error. Therefore, the ratio $\frac{\vartheta_{i,\mathfrak{h}}}{\vartheta_{\mathfrak{h}}} \geq 1$ is an appropriate measure of disagreement.

Since the Resetting Forecast $E^*_q\pi^{av}_{q+\mathfrak{h}}$ and the Average Forecast $\mathcal{F}_q\pi^{av}_{q+\mathfrak{h}} = \int_0^1 \mathcal{F}_{i,q}\pi^{av}_{q+\mathfrak{h}}$ are not biased, forecasting dominance is equivalent to having the smallest variance of forecast errors. Therefore, knowing estimates for the DGP parameters $\left(\rho_{\mathfrak{h}}, \bar{\sigma}^2\right)$, rigidity parameters $\gamma_{\mathfrak{h}}$, and noise variances $\left(\sigma^2_{\upsilon,\mathfrak{h}}, \sigma^2_{\eta,\mathfrak{h}}\right)$ is enough for telling whether the Resetting Forecast dominates the Average Forecast, i.e. if $\vartheta^*_{q,\mathfrak{h}} < \vartheta_{q,\mathfrak{h}}$.

However, estimates for the noise variances $\left(\sigma^2_{\upsilon,\mathfrak{h}}, \sigma^2_{\eta,\mathfrak{h}}\right)$ are not readily obtainable from survey microdata, as forecasters only reveal values for $\mathcal{F}_{i,q}\pi^{av}_{q+\mathfrak{h}}$ and not their initial raw forecasts $E^*_{i,q}\pi^{av}_{q+\mathfrak{h}}$. Therefore, even though the econometrician estimates $\vartheta_{q,\mathfrak{h}}$, she cannot infer $\vartheta^*_{q,\mathfrak{h}} = \sigma^2_{\eta,\mathfrak{h}}$.

For coping with this issue, only using statistics easily obtainable from the time series of CPI inflation and SPF microdata of individual forecasts, the following proposition provides an equivalent condition to verify whether Resetting Forecasts dominate Average Forecasts. More specifically, a few sufficient statistics, i.e. $\vartheta_{i,\mathfrak{h}}$, $\vartheta_{\mathfrak{h}}$ and $\bar{\sigma}^2$, are enough to verify dominance. And estimates of those variances are very easy to obtain from the realized quarterly average price rates of CPI inflation and SPF microdata.

The basic message of the proposition is that Resetting Forecasts dominate Average Forecasts when disagreement is sufficiently large, but not excessively large so that forecast efficiency is compromised. For reasons better explained further on, we call the conditions leading to the disagreement lower and upper bounds as the *harmonic* and *efficiency conditions*.

Proposition 2 *Consider the modelling assumptions and results presented in Sections 5.1 and 5.2. In this case, the Resetting Forecast* $E_q^* \pi_{q+\mathfrak{h}}^{av}$ *has better forecasting performance than the Average Forecast* $\mathcal{F}_q \pi_{q+\mathfrak{h}}^{av}$ *if and only if disagreement* $\frac{\vartheta_{i,\mathfrak{h}}}{\vartheta_\mathfrak{h}}$ *satisfies the following condition:*

$$\frac{2}{\left[1 + \left(\bar{\sigma}^2/\vartheta_\mathfrak{h}\right)^{-1}\right]} < \frac{\vartheta_{i,\mathfrak{h}}}{\vartheta_\mathfrak{h}} < \frac{\bar{\sigma}^2}{\vartheta_\mathfrak{h}} \tag{13}$$

The proof is shown in Appendix D.

The right-hand inequality $\frac{\vartheta_{i,\mathfrak{h}}}{\vartheta_\mathfrak{h}} < \frac{\bar{\sigma}^2}{\vartheta_\mathfrak{h}}$ has the intuition of an *efficiency condition*, as the variance of Individual Forecast errors $\vartheta_{i,\mathfrak{h}}$ should be smaller than the unconditional variance of inflation $\bar{\sigma}^2$. Otherwise, individuals would be better-off by simply using the inflation unconditional mean as their forecast. The left-hand inequality $\frac{2}{\left[1+\left(\bar{\sigma}^2/\vartheta_\mathfrak{h}\right)^{-1}\right]} < \frac{\vartheta_{i,\mathfrak{h}}}{\vartheta_\mathfrak{h}}$ is the *harmonic condition*, as it states that disagreement $\frac{\vartheta_{i,\mathfrak{h}}}{\vartheta_\mathfrak{h}}$ should be larger than the harmonic mean between unity and the efficiency limit $\frac{\bar{\sigma}^2}{\vartheta_\mathfrak{h}}$.

Note that, if there is no disagreement (i.e. $\frac{\vartheta_{i,\mathfrak{h}}}{\vartheta_\mathfrak{h}} = 1$), the Resetting Forecast never dominates the Average Forecast. Otherwise, there will be an analytical contradiction, for the efficiency condition implies $\vartheta_\mathfrak{h} < \bar{\sigma}^2$, while the harmonic condition implies the opposite, i.e. $\vartheta_\mathfrak{h} > \bar{\sigma}^2$.

5.2.1 Testing Theoretical Forecast Dominance

We highlight the result (13) is obtained using a simplified DGP process for inflation, and assuming forecasts are unbiased and the main friction governing forecasts formation comes from noisy-dispersed information. Nonetheless, the advantage of Proposition 2 is proposing a fast way to suggest which horizons the Resetting Forecast dominates the Aggregate Forecasts before estimating the forecast model and formally testing its forecast performance, as carried out in Sections 3.1 and 4. Using result (13), all we need to verify the dominance are three variance estimates, easily recovered from CPI average price rates and the microdata of SPF individual forecasts: (i) sample variance of Individual Forecast errors $\hat{\vartheta}_{i,\mathfrak{h}}$; (ii) sample variance of Average Forecast errors $\hat{\vartheta}_\mathfrak{h}$;

and (iii) sample variance of CPI average price rates $\hat{\bar{\sigma}}^2$. Here, hatted parameters indicate sample estimates.

Therefore, in this section, we test whether result (13) can provide us with the same massage that we obtained in Section 4, in terms of informing us the horizons in which Resetting Forecasts have smaller variance of forecast errors than those of Average Forecasts. By construction, result (13) does not tells us how strong forecast dominance are, but rather serves as an indication of whether there are forecast dominance. Since the sample variances $\hat{\vartheta}_{i,\mathfrak{h}}$, $\hat{\vartheta}_{\mathfrak{h}}$, and $\hat{\bar{\sigma}}^2$ are not used in the exercises shown in Sections 3.1 and 4, the analyses carried out with (13) are independent of those shown in the previous sections.

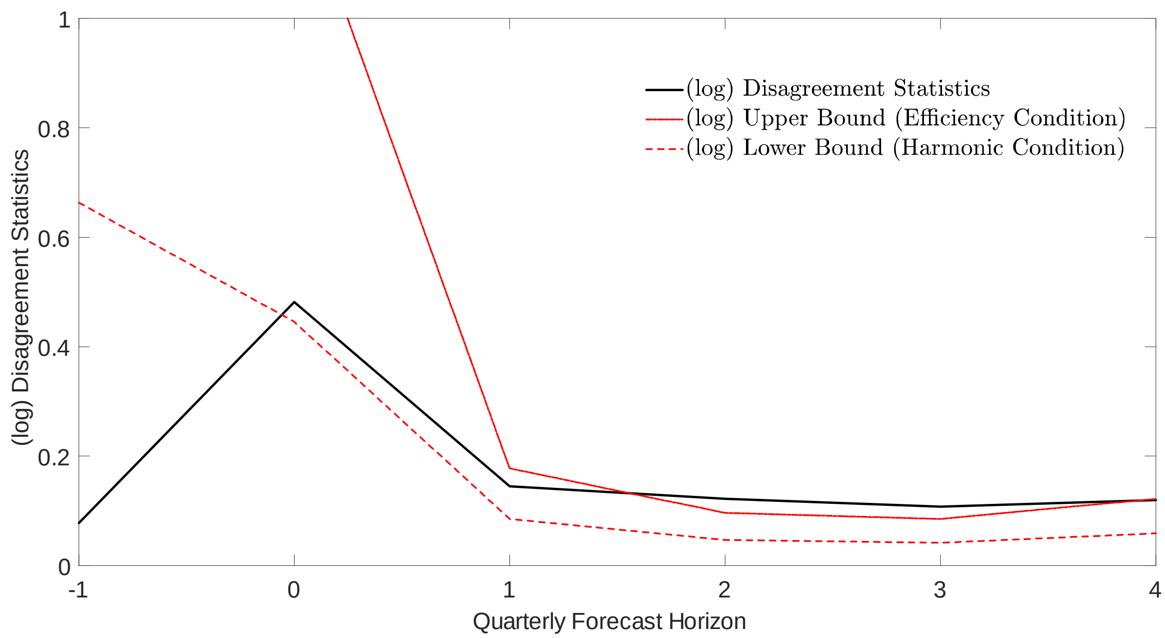

Figure 4: Forecast Dominance Implied by Disagreement

Notes: Forecast Performance Exercise based on Proposition 2, using disagreement metrics from microdata of SPF individual forecasts for CPI inflation.

Figure 4 draws the (log) disagreement statistics $\frac{\hat{\vartheta}_{i,\mathfrak{h}}}{\hat{\vartheta}_{\mathfrak{h}}}$ along with the (log) upper and lower bounds implied by the efficiency and disagreement conditions defined in (13). The sample variances are retrieved from CPI average price rates and the microdata of SPF individual forecasts, using the same effective testing window used in Section 4: 2006:Q1 to 2023:Q2. Since results (10), (12) and (13) are obtained under the assumption that forecasts are unbiased, we demeaned the individual forecasts errors before computing the statistics.[24]

[24] Allowing for biased forecasts requires adjusting those three systems, without changing much the analytical and

Note the conclusions are in line with the Relative MSE's for $\pi^{av^*}_{t,t+h}$, shown in Tables 3 to 6 in Section 4, specially in exercises with unrestricted models. That is, Resetting Forecasts errors have smaller variances for nowcasts ($\mathfrak{h} = 0$), 1-quarter ahead forecasts ($\mathfrak{h} = 1$) and 4-quarter ahead forecasts ($\mathfrak{h} = 4$), as disagreement $\frac{\hat{\vartheta}_{i,\mathfrak{h}}}{\hat{\vartheta}_{\mathfrak{h}}}$ lies inside the theoretical interval. For 2-quarter and 3-quater ahead forecasts, disagreement is located slightly above the interval upper bound, whereas it lies well below the interval lower bound for backcasts.

6 Conclusions

Professional inflation forecasts contain valuable information obscured by information frictions that vary systematically across forecast horizons. By explicitly modeling these horizon-specific frictions, we extract improved forecasts that significantly outperform Survey of Professional Forecasters consensus nowcasts while matching performance at longer horizons.

Our results establish three main findings. First, forecast rigidity increases sharply with horizon length, rising from essentially zero for backcasts to 0.81 beyond two quarters. Models imposing either rational expectations or uniform rigidity across horizons are strongly rejected and fail to improve upon survey averages. Second, accounting for this heterogeneity yields substantial gains: our Resetting Nowcasts reduce mean squared errors by 50 percent relative to SPF averages in pseudo-real-time tests. Third, we provide a tractable theoretical framework that predicts when such improvements will emerge based on three sufficient statistics computed from survey microdata.

The theoretical criterion reveals that improved forecasts dominate when disagreement among individual forecasters lies within an optimal interval—large enough to signal meaningful information dispersion but not so large that forecasts become unreliable. Applied to SPF data, these microdata-based bounds correctly predict the horizons where our approach succeeds, suggesting the method generalizes readily to other surveys and variables.

Our inflation decomposition also offers policy-relevant insights. The 2021-2023 inflation surge primarily reflected medium-run transitory components rather than permanent shifts in trend inflation, with implications for appropriate monetary policy responses.

These findings open several avenues for future research. First, extending the framework to incorporate real-time data flow and forecast updates could further enhance nowcasting performance.

empirical results we obtain.

Second, applying the approach to other macroeconomic variables—such as GDP growth, unemployment, or financial market indicators—would test the method's broader applicability. Third, investigating whether combining our Resetting Forecasts with machine learning techniques or high-frequency data could yield additional gains remains an open question. Finally, understanding how forecast frictions evolve during periods of structural change or regime shifts could improve real-time policy analysis during economic turbulence.

The practical value of our approach lies in its simplicity and generalizability. Policymakers and forecasters can use readily available survey microdata to identify which forecast horizons offer the greatest potential for improvement before investing in more elaborate modeling efforts. This provides a cost-effective screening tool for allocating resources toward the most promising forecasting enhancements across different variables and time horizons.

References

AIOLFI, M., C. CAPISTRAN, AND A. TIMMERMANN (2012): "Forecast Combinations," in *The Oxford Handbook of Economic Forecasting*, pp. 355–388. Oxford University Press, 1 edn.

ANDRADE, P., R. K. CRUMP, S. EUSEPI, AND E. MOENCH (2016): "Fundamental disagreement," *Journal of Monetary Economics*, 83(C), 106–128.

ANDRADE, P., AND H. LE BIHAN (2013): "Inattentive professional forecasters," *Journal of Monetary Economics*, 60(8), 967–982.

ANDREWS, D. W. K., AND J. C. MONAHAN (1992): "An Improved Heteroskedasticity and Autocorrelation Consistent Covariance Matrix Estimator," *Econometrica*, 60(4), 953–966.

ANG, A., G. BEKAERT, AND M. WEI (2007): "Do macro variables, asset markets, or surveys forecast inflation better?," *Journal of Monetary Economics*, 54(4), 1163–1212.

AREOSA, M. B. M., W. D. AREOSA, AND V. CARRASCO (2020): "A sticky-dispersed information Phillips Curve: a model with partial and delayed information," *Macroeconomic Dynamics*, 24(4), 747–773.

BEVERIDGE, S., AND C. R. NELSON (1981): "A new approach to decomposition of economic time series into permanent and transitory components with particular attention to measurement of the 'business cycle'," *Journal of Monetary Economics*, 7(2), 151–174.

Capistran, C., and A. Timmermann (2009a): "Disagreement and Biases in Inflation Expectations," *Journal of Money, Credit and Banking*, 41(2-3), 365–396.

——— (2009b): "Forecast Combination With Entry and Exit of Experts," *Journal of Business & Economic Statistics*, 27(4), 428–440.

Cogley, T., and A. M. Sbordone (2008): "Trend Inflation, Indexation, and Inflation Persistence in the New Keynesian Phillips Curve," *American Economic Review*, 98(5), 2101–2126.

Coibion, O., and Y. Gorodnichenko (2012): "What Can Survey Forecasts Tell Us about Information Rigidities?," *Journal of Political Economy*, 120(1), 116–159.

——— (2015): "Information Rigidity and the Expectations Formation Process: A Simple Framework and New Facts," *American Economic Review*, 105(8), 2644–2678.

Croushore, D. (2010): "An Evaluation of Inflation Forecasts from Surveys Using Real-Time Data," *The B.E. Journal of Macroeconomics*, 10(1).

Croushore, D., and T. Stark (2019): "Fifty Years of the Survey of Professional Forecasters," *Economic Insights, Federal Reserve Bank of Philadelphia*, 4(4).

Crump, R. K., S. Eusepi, D. O. Lucca, and E. Moench (2014): "Data insight: which growth rate? It's a weighty subject," Liberty Street Economics December 2014, Federal Reserve Bank of New York.

Dahlhaus, T., J.-D. Guenette, and G. Vasishtha (2017): "Nowcasting BRIC+M in real time," *International Journal of Forecasting*, 33(4), 915–935.

Del Negro, M., and S. Eusepi (2011): "Fitting observed inflation expectations," *Journal of Economic Dynamics and Control*, 35(12), 2105–2131.

Diebold, F. X., and R. S. Mariano (1995): "Comparing Predictive Accuracy," *Journal of Business & Economic Statistics*, 13(3), 253–263.

Durbin, J., and S. J. Koopman (2012): *Time Series Analysis by State Space Methods*, no. 38 in Oxford Statistical Science. Oxford University Press, 2nd edn., 02403.

Faust, J., and J. H. Wright (2009): "Comparing Greenbook and Reduced Form Forecasts Using a Large Realtime Dataset," *Journal of Business & Economic Statistics*, 27(4), 468–479.

——— (2013): "Forecasting Inflation," in *Handbook of Economic Forecasting*, vol. 2, Part A, pp. 2–56. Elsevier.

Giacomini, R., and H. White (2006): "Tests of Conditional Predictive Ability," *Econometrica*, 74(6), 1545–1578.

Greenlees, J. S., and C. C. Mason (1996): "Overview of the 1998 Revision of the Consumer Price Index," Monthly Labor Review December 1996, U.S. Bureau of Labor Statistics.

Harrison, J., and M. West (1997): *Bayesian forecasting and dynamic models*. Springer, New York.

Harrison, P. J., and C. F. Stevens (1975): "Bayes forecasting in action: case studies," Department of Statistics Warwick Research Report 14, University of Warwick.

Jain, M. (2018): "Sluggish Forecasts," *Bank of Canada Staff Working Paper*, (2018-39).

Knotek II, E. S., and S. Zaman (2017): "Nowcasting U.S. Headline and Core Inflation," *Journal of Money, Credit and Banking*, 49(5), 931–968.

Lucas, R. E. (1976): "Econometric policy evaluation: A critique," *Carnegie-Rochester Conference Series on Public Policy*, 1, 19–46.

Mackowiak, B., and M. Wiederholt (2009): "Optimal Sticky Prices under Rational Inattention," *American Economic Review*, 99(3), 769–803.

Mankiw, N. G., and R. Reis (2002): "Sticky Information versus Sticky Prices: A Proposal to Replace the New Keynesian Phillips Curve," *The Quarterly Journal of Economics*, 117(4), 1295–1328.

Marcellino, M., J. H. Stock, and M. W. Watson (2006): "A comparison of direct and iterated multistep AR methods for forecasting macroeconomic time series," *Journal of Econometrics*, 135(1), 499–526.

Mariano, R. S., and Y. Murasawa (2003): "A new coincident index of business cycles based on monthly and quarterly series," *Journal of Applied Econometrics*, 18(4), 427–443.

McCracken, M. W., and J. T. McGillicuddy (2018): “An empirical investigation of direct and iterated multistep conditional forecasts,” *Journal of Applied Econometrics*, 34(2), 181–204.

Mertens, E., and J. M. Nason (2018): “Inflation and professional forecast dynamics: an evaluation of stickiness, persistence, and volatility,” BIS Working Papers 713, Bank for International Settlements.

Monti, F. (2010): “Combining Judgment and Models,” *Journal of Money, Credit and Banking*, 42(8), 1641–1662.

Nason, J. M., and G. W. Smith (2013): “Reverse Kalman filtering U.S. inflation with sticky professional forecasts,” Discussion Paper 13-34, Federal Reserve Bank of Philadelphia.

Patton, A. J., and A. Timmermann (2010): “Why do forecasters disagree? Lessons from the term structure of cross-sectional dispersion,” *Journal of Monetary Economics*, 57(7), 803–820.

——— (2011): “Predictability of Output Growth and Inflation: A Multi-Horizon Survey Approach,” *Journal of Business & Economic Statistics*, 29(3), 397–410.

Prado, R., and M. West (2010): *Time series*. Chapman & Hall, London, 00083.

Rossi, B., and T. Sekhposyan (2015): “Macroeconomic Uncertainty Indices Based on Nowcast and Forecast Error Distributions,” *American Economic Review*, 105(5), 650–655.

Schmitt-Grohe, S., and M. Uribe (2022): “What Do Long Data Tell Us About the Inflation Hike Post COVID-19 Pandemic?,” *NBER Working Papers*.

Sims, C. A. (2003): “Implications of rational inattention,” *Journal of Monetary Economics*, 50(3), 665–690.

Stock, J. H., and M. W. Watson (2007): “Why Has U.S. Inflation Become Harder to Forecast?,” *Journal of Money, Credit and Banking*, 39(s1), 3–33.

——— (2010): “Modeling Inflation After the Crisis,” NBER Working Papers 16488, National Bureau of Economic Research, Inc.

Woodford, M. (2003): “Imperfect Common Knowledge and the Effects of Monetary Policy,” in *Knowledge, Information and Expectations in Modern Macroeconomics: Macroeconomics: In*

Honor of Edmund S. Phelps, edited by Philippe Aghion, Roman Frydman, Joseph Stiglitz, and Michael Woodford, pp. 25–58. Princeton: Princeton University Press.

A Average-Price Rate

We aim to derive a log-linearized map between $\Pi_t^{av}$and Π_t. For that, lower case variables correspond to log-linearized versions of the original upper case variables, e.g. $\varkappa_t \equiv \log(\mathcal{X}_t)$. Therefore, we have $\pi_t = p_t - p_{t-1}$ and $\pi_t^{av} = p_t^{av} - p_{t-3}^{av}$. As for P_t^{av}, we must use a first-order log-approximation centered at P_t:

$$\begin{aligned} P_t\left[p_t^{av} - \log(P_t)\right] \approx & \quad \tfrac{1}{3} P_t\left(\left[p_{t+1} - \log(P_t)\right] + \left[p_t - \log(P_t)\right] + \left[p_{t-1} - \log(P_t)\right]\right) \\ \therefore p_t^{av} \approx & \quad \tfrac{1}{3}\left(p_{t+1} + p_t + p_{t-1}\right) \end{aligned}$$

which implies $\pi_t^{av} \approx \frac{1}{3}\left(p_{t+1} + p_t + p_{t-1}\right) - \frac{1}{3}\left(p_{t-2} + p_{t-3} + p_{t-4}\right)$. Since $\pi_t = p_t - p_{t-1}$, we obtain $\pi_t^{av} \approx \frac{1}{3}\left[\pi_{t+1} + 2\pi_t + 3\pi_{t-1} + 2\pi_{t-2} + \pi_{t-3}\right]$.

B Forecast Dynamics for Longer Horizons

Proposition 1 *If the degree of forecast rigidity for any horizon $h \geq H + 3$ is constant, with $H \geq 0$, and there is no extra information disturbances for those longer horizons, i.e. $\alpha_h = \bar{\alpha}$ and $s_{h,t}^{av} = 0$ for $h \in \{H+3, H+6, ...\}$, then $F_t \pi_{t+h}^{av}$ evolves according to an autoregressive system that does not depend on lagged forecasts for longer horizons:*

$$\begin{aligned} \mathcal{F}_t \pi_{t+h}^{av} &= \mathcal{F}_t \pi_{t+h}^{amr.} + \mathcal{F}_t \pi_{t+h}^{asr} + \mathcal{F}_t \pi_{t+h}^{alr} \\ &\text{where} \\ \mathcal{F}_t \pi_{t+h}^{amr.} &= (1-\bar{\alpha})\, E_{t-2} \pi_{t+h}^{amr} + \bar{\alpha}\left(\rho_{mr}\right)^3 \mathcal{F}_{t-3} \pi_{t-3+h}^{amr} \\ \mathcal{F}_t \pi_{t+h}^{asr.} &= (1-\bar{\alpha})\, E_{t-2} \pi_{t+h}^{asr} + \bar{\alpha}\left(\rho_{sr}\right)^3 \mathcal{F}_{t-3} \pi_{t-3+h}^{asr} \\ \mathcal{F}_t \pi_{t+h}^{alr} &= (1-\bar{\alpha})\, E_{t-2} \pi_{t+h}^{alr} + \bar{\alpha} \mathcal{F}_{t-3} \pi_{t-3+h}^{alr} \\ \pi_{t+h}^{amr} &\equiv \tfrac{1}{3}\left[\pi_{t+h+1}^{mr} + 2\pi_{t+h}^{mr} + 3\pi_{t+h-1}^{mr} + 2\pi_{t+h-2}^{mr} + \pi_{t+h-3}^{mr}\right] \\ \pi_{t+h}^{asr} &\equiv \tfrac{1}{3}\left[\pi_{t+h+1}^{sr} + 2\pi_{t+h}^{sr} + 3\pi_{t+h-1}^{sr} + 2\pi_{t+h-2}^{sr} + \pi_{t+h-3}^{sr}\right] \\ \pi_{t+h}^{alr} &\equiv \tfrac{1}{3}\left[\pi_{t+h+1}^{lr} + 2\pi_{t+h}^{lr} + 3\pi_{t+h-1}^{lr} + 2\pi_{t+h-2}^{lr} + \pi_{t+h-3}^{lr}\right] \end{aligned}$$

Proof If $\alpha_h = \bar{\alpha}$ and $\mathfrak{s}_{h,t} = 0$ for $h \in \{H+3, H+6, ...\}$ and $H \geq 0$, with a forecast rule $E_t^* \pi_{t+h}^{av} = E_{t-2}\pi_{t+h}^{av} + \mathfrak{s}_{h,t}$, then the law of motion of the aggregate forecast is described as $\mathcal{F}_t \pi_{t+h}^{av} = (1-\bar{\alpha}) E_{t-2}\pi_{t+h}^{av} + \bar{\alpha}\mathcal{F}_{t-3}\pi_{t+h}^{av}$. Using the lag operator (L), we can expand the equation as follows:

$$\begin{aligned}
\mathcal{F}_t \pi_{t+h}^{av} &= (1-\bar{\alpha}) E_{t-2}\pi_{t+h}^{av} + \bar{\alpha}\mathcal{F}_{t-3}\pi_{t+h}^{av} = (1-\bar{\alpha}) E_{t-2}\pi_{t+h}^{av} + \bar{\alpha} L^3 \mathcal{F}_t \pi_{t+h+3}^{av} \\
&= (1-\bar{\alpha}) E_{t-2}\pi_{t+h}^{av} + (1-\bar{\alpha})\bar{\alpha} E_{t-5}\pi_{t+h}^{av} + \bar{\alpha}^2 L^6 \mathcal{F}_t \pi_{t+h+6}^{av} \\
&= (1-\bar{\alpha}) E_{t-2}\pi_{t+h}^{av} + (1-\bar{\alpha})\bar{\alpha} E_{t-5}\pi_{t+h}^{av} + (1-\bar{\alpha})\bar{\alpha}^2 E_{t-8}\pi_{t+h}^{av} + \bar{\alpha}^3 L^9 \mathcal{F}_t \pi_{t+h+9}^{av} \\
&= ...
\end{aligned}$$

Therefore, we obtain:

$$\mathcal{F}_t \pi_{t+h}^{av} = (1-\bar{\alpha})\left(E_{t-2}\pi_{t+h}^{av}\right) + (1-\bar{\alpha})\sum_{v=1}^{\infty}(\bar{\alpha})^v E_{(t-2-3v)}\pi_{t+h}^{av} = (1-\bar{\alpha})\sum_{v=0}^{\infty}(\bar{\alpha})^v E_{(t-2-3v)}\pi_{t+h}^{av}$$

where:

$$\begin{aligned}
E_{(t-2-3v)}\pi_{t+h}^{av} &= E_{(t-2-3v)}\tfrac{1}{3}\left[\pi_{t+h+1}^{sa} + 2\pi_{t+h}^{sa} + 3\pi_{t+h-1}^{sa} + 2\pi_{t+h-2}^{sa} + \pi_{t+h-3}^{sa}\right] \\
&= E_{(t-2-3v)}\tfrac{1}{3}\left[\pi_{t+h+1}^{mr} + 2\pi_{t+h}^{mr} + 3\pi_{t+h-1}^{mr} + 2\pi_{t+h-2}^{mr} + \pi_{t+h-3}^{mr}\right] \\
&\quad + E_{(t-2-3v)}\tfrac{1}{3}\left[\pi_{t+h+1}^{sr} + 2\pi_{t+h}^{sr} + 3\pi_{t+h-1}^{sr} + 2\pi_{t+h-2}^{sr} + \pi_{t+h-3}^{sr}\right] \\
&\quad + E_{(t-2-3v)}\tfrac{1}{3}\left[\pi_{t+h+1}^{lr} + 2\pi_{t+h}^{lr} + 3\pi_{t+h-1}^{lr} + 2\pi_{t+h-2}^{lr} + \pi_{t+h-3}^{lr}\right]
\end{aligned}$$

Up to this point, the result is general and does not require $H \geq 0$. However, in order to proceed we must know whether period $(t-2-3v)$ belongs to the past or future of each inflation timing in the last result, from $(t+h-3)$ to $(t+h+1)$. Now, using the assumptions $h \geq H+3$ and $H \geq 0$, we show below that $(t-2-3v)$ is actually smaller than the smallest timing $(t+h-3)$. Indeed, notice that $(t+h-3) \geq (t+H+3-3) = (t+H) \geq t \geq t-2-3v$. With that result, it makes it easier to compute expectations when considering the DGP dynamic equations:

$$\begin{aligned}
&\pi_t^{sa} = \pi_t^{mr} + \pi_t^{sr} + \pi_t^{lr} \quad ; \; \pi_t^{mr} = \rho_{mr}\pi_{t-1}^{mr} + \varepsilon_t^{mr} \\
&\pi_t^{lr} = \pi_{t-1}^{lr} + \varepsilon_t^{lr} \qquad\qquad ; \; \pi_t^{sr} = \rho_{sr}\pi_{t-1}^{sr} + \varepsilon_t^{sr}
\end{aligned}$$

Their dynamics imply that:

$$\begin{aligned}
E_{(t-2-3v)}\pi_{t+h}^{av} &= (\rho_{mr})^{h-1+3v}\tfrac{1}{3}\left[(\rho_{mr})^4 + 2(\rho_{mr})^3 + 3(\rho_{mr})^2 + 2(\rho_{mr}) + 1\right]\pi_{t-2-3v}^{mr} \\
&\quad + (\rho_{sr})^{h-1+3v}\tfrac{1}{3}\left[(\rho_{sr})^4 + 2(\rho_{sr})^3 + 3(\rho_{sr})^2 + 2(\rho_{sr}) + 1\right]\pi_{t-2-3v}^{mr} \\
&\quad + \tfrac{1}{3}\left[1+2+3+2+1\right]\pi_{t-2-3v}^{lr}
\end{aligned}$$

Since $\mathcal{F}_t\pi^{av}_{t+h} = (1-\bar{\alpha})\sum_{v=0}^{\infty}(\bar{\alpha})^v E_{(t-2-3v)}\pi^{av}_{t+h}$, we decompose $\mathcal{F}_t\pi^{av}_{t+h}$ into three terms:

$$\mathcal{F}_t\pi^{av}_{t+h} = \mathcal{F}_t\pi^{amr.}_{t+h} + \mathcal{F}_t\pi^{asr}_{t+h} + \mathcal{F}_t\pi^{alr}_{t+h}$$

where

$$\begin{aligned}
\mathcal{F}_t\pi^{amr.}_{t+h} &= \tfrac{(1-\bar{\alpha})\Phi_{h,h}}{3}\sum_{v=0}^{\infty}\left(\bar{\alpha}\left(\rho_{mr}\right)^3\right)^v \pi^{mr}_{t-2-3v} \\
\mathcal{F}_t\pi^{asr}_{t+h} &= \tfrac{(1-\bar{\alpha})\Phi_{l,h}}{3}\sum_{v=0}^{\infty}\left(\bar{\alpha}\left(\rho_{sr}\right)^3\right)^v \pi^{sr}_{t-2-3v} \\
\mathcal{F}_t\pi^{alr}_{t+h} &= \tfrac{(1-\bar{\alpha})\Phi_{lr}}{3}\sum_{v=0}^{\infty}\left(\bar{\alpha}\right)^v \pi^{lr}_{t-2-3v}
\end{aligned}$$

and $\Phi_{h,h}$, $\Phi_{l,h}$ and Φ_{lr} are auxiliary parameters:

$$\begin{aligned}
\Phi_{h,h} &= \left(\rho_{mr}\right)^{h-1}\left[\left(\rho_{mr}\right)^4 + 2\left(\rho_{mr}\right)^3 + 3\left(\rho_{mr}\right)^2 + 2\left(\rho_{mr}\right) + 1\right] = \left(\rho_{mr}\right)^{h-1}\left[\left(\rho_{mr}\right)^2 + \left(\rho_{mr}\right) + 1\right]^2 \\
\Phi_{l,h} &= \left(\rho_{sr}\right)^{h-1}\left[\left(\rho_{sr}\right)^4 + 2\left(\rho_{sr}\right)^3 + 3\left(\rho_{sr}\right)^2 + 2\left(\rho_{sr}\right) + 1\right] = \left(\rho_{sr}\right)^{h-1}\left[\left(\rho_{sr}\right)^2 + \left(\rho_{sr}\right) + 1\right]^2 \\
\Phi_{lr} &= [1+2+3+2+1] = 9
\end{aligned}$$

We can work on those components as follows:

$$\begin{aligned}
\mathcal{F}_t\pi^{amr.}_{t+h} &= \tfrac{(1-\bar{\alpha})\Phi_{h,h}}{3}\sum_{v=0}^{\infty}\left(\bar{\alpha}\left(\rho_{mr}\right)^3\right)^v \pi^{mr}_{t-2-3v} \\
&= \tfrac{(1-\bar{\alpha})\Phi_{h,h}}{3}\pi^{mr}_{t-2} + \tfrac{(1-\bar{\alpha})\Phi_{h,h}}{3}\sum_{v=1}^{\infty}\left(\bar{\alpha}\left(\rho_{mr}\right)^3\right)^v \pi^{mr}_{t-2-3v} \\
&= \tfrac{(1-\bar{\alpha})\Phi_{h,h}}{3}\pi^{mr}_{t-2} + \bar{\alpha}\left(\rho_{mr}\right)^3 \overbrace{\frac{(1-\bar{\alpha})\Phi_{h,h}}{3}\sum_{V=0}^{\infty}\left(\bar{\alpha}\left(\rho_{mr}\right)^3\right)^V \pi^{mr}_{(t-3)-2-3V}}^{V=v-1} \\
&= \tfrac{(1-\bar{\alpha})\Phi_{h,h}}{3}\pi^{mr}_{t-2} + \bar{\alpha}\left(\rho_{mr}\right)^3 \mathcal{F}_{(t-3)}\pi^{amr}_{(t-3)+h}
\end{aligned}$$

Analogously, we have:

$$\begin{aligned}
\mathcal{F}_t\pi^{asr.}_{t+h} &= \tfrac{(1-\bar{\alpha})\Phi_{l,h}}{3}\pi^{sr}_{t-2} + \bar{\alpha}\left(\rho_{sr}\right)^3 \mathcal{F}_{(t-3)}\pi^{asr}_{(t-3)+h} \\
\mathcal{F}_t\pi^{alr}_{t+h} &= \tfrac{(1-\bar{\alpha})\Phi_{lr}}{3}\pi^{lr}_{t-2} + \bar{\alpha}\left(\rho_{sr}\right)^3 \mathcal{F}_{(t-3)}\pi^{lr}_{(t-3)+h}
\end{aligned}$$

Using the definitions of $\Phi_{h,h}$, $\Phi_{l,h}$ and Φ_{lr}, note now that

$$\begin{aligned}
\tfrac{\Phi_{h,h}\pi^{mr}_{t-2}}{3} &= \tfrac{1}{3}\left(\rho_{mr}\right)^{h-1}\left[\left(\rho_{mr}\right)^4 + 2\left(\rho_{mr}\right)^3 + 3\left(\rho_{mr}\right)^2 + 2\left(\rho_{mr}\right) + 1\right]\pi^{mr}_{t-2} \\
&= \tfrac{1}{3}\left[\left(\rho_{mr}\right)^{h+3}\pi^{mr}_{t-2} + 2\left(\rho_{mr}\right)^{h+2}\pi^{mr}_{t-2} + 3\left(\rho_{mr}\right)^{h+1}\pi^{mr}_{t-2} + 2\left(\rho_{mr}\right)^{h}\pi^{mr}_{t-2} + \left(\rho_{mr}\right)^{h-1}\pi^{mr}_{t-2}\right] \\
&= \tfrac{1}{3}E_{t-2}\left[\pi^{mr}_{t+h+1} + 2\pi^{mr}_{t+h} + 3\pi^{mr}_{t+h-1} + 2\pi^{mr}_{t+h-2} + \pi^{mr}_{t+h-3}\right] = E_{t-2}\pi^{amr}_{t+h}
\end{aligned}$$

Analogously, we have $\frac{\Phi_{l,h}}{3}\pi^{sr}_{t-2} = E_{t-2}\pi^{asr}_{t+h}$ and $\frac{\Phi_{lr}}{3}\pi^{lr}_{t-2} = E_{t-2}\pi^{alr}_{t+h}$. Therefore, under the assumed conditions, the dynamics of $\mathcal{F}_t\pi^{av}_{t+h}$ can be described as follows:

$$
\begin{aligned}
\mathcal{F}_t\pi^{av}_{t+h} &= \mathcal{F}_t\pi^{amr.}_{t+h} + \mathcal{F}_t\pi^{asr}_{t+h} + \mathcal{F}_t\pi^{alr}_{t+h} \\
\mathcal{F}_t\pi^{amr.}_{t+h} &= (1-\bar{\alpha})\, E_{t-2}\pi^{amr}_{t+h} + \bar{\alpha}\,(\rho_{mr})^3\, \mathcal{F}_{t-3}\pi^{amr}_{t-3+h} \\
\mathcal{F}_t\pi^{asr.}_{t+h} &= (1-\bar{\alpha})\, E_{t-2}\pi^{asr}_{t+h} + \bar{\alpha}\,(\rho_{sr})^3\, \mathcal{F}_{t-3}\pi^{asr}_{t-3+h} \\
\mathcal{F}_t\pi^{alr}_{t+h} &= (1-\bar{\alpha})\, E_{t-2}\pi^{alr}_{t+h} + \bar{\alpha}\mathcal{F}_{t-3}\pi^{alr}_{t-3+h}
\end{aligned}
$$

$$
\begin{aligned}
\pi^{amr}_{t+h} &\equiv \tfrac{1}{3}\left[\pi^{mr}_{t+h+1} + 2\pi^{mr}_{t+h} + 3\pi^{mr}_{t+h-1} + 2\pi^{mr}_{t+h-2} + \pi^{mr}_{t+h-3}\right] \\
\pi^{asr}_{t+h} &\equiv \tfrac{1}{3}\left[\pi^{sr}_{t+h+1} + 2\pi^{sr}_{t+h} + 3\pi^{sr}_{t+h-1} + 2\pi^{sr}_{t+h-2} + \pi^{sr}_{t+h-3}\right] \\
\pi^{alr}_{t+h} &\equiv \tfrac{1}{3}\left[\pi^{lr}_{t+h+1} + 2\pi^{lr}_{t+h} + 3\pi^{lr}_{t+h-1} + 2\pi^{lr}_{t+h-2} + \pi^{lr}_{t+h-3}\right]
\end{aligned}
$$

C Estimated Forecast System

As for the zero-meaned monthly complementary forecasting components $\mathfrak{s}_{h,t}$, which we model as white-noise components, we need an extra assumption for very distant horizons. Recall that $h = 12$ is the furthest horizon for which we have observed SPF quarterly forecasts, i.e. for $\mathcal{F}_t\pi^{av}_{t+12}$. At this horizon, the aggregate component $\mathfrak{s}^{av}_{12,t}$ depends on complementary forecasting components from $\mathfrak{s}_{9,t}$ to $\mathfrak{s}_{13,t}$. Therefore, we impose $\mathfrak{s}_{h,t} = 0$ for $\forall h \geq 14$ in order for $\mathfrak{s}_{13,t}$ to be the furthest complementary forecasting component whose distribution will be retrieved by the Kalman filter during estimation. In the same line, we impose a similar restriction for distant past horizons. Since we observe $\mathcal{F}_t\pi^{av}_{t-3}$, the aggregate component $\mathfrak{s}^{av}_{-3,t}$ depends on complementary forecasting components from $\mathfrak{s}_{-2,t}$ to $\mathfrak{s}_{-6,t}$. At the pivot month t, however, the previous quarter regards months $(t-2)$ to $(t-4)$. Therefore, we assume $\mathfrak{s}_{h,t} = 0$ for $\forall h \leq -5$. That is, we only allow for non-zero components $\mathfrak{s}_{h,t}$ at quarterly horizons surveyed by SPF. In a nutshell, we impose $\mathfrak{s}_{h,t} = 0$ for $\forall h \geq 14$ and $\forall h \leq -5$.

For identification purposes, we also impose that monthly forecasting components related to the same SPF quarterly horizon are equal. That is, for any horizon $h \in \{-3, 0, 3, 6, 9, 12\}$, we set $\mathfrak{s}_{h+1,t} = \mathfrak{s}_{h,t}$ and $\mathfrak{s}_{h-1,t} = \mathfrak{s}_{h,t}$. Lastly, for inference pragmatism, we need assumptions to simplify estimation in this mixed-frequency estimation environment, as SPF information is much more sparse than monthly information. Even though $\mathfrak{s}_{h,t}$ varies in time and is different for each horizon, we assume all of them have the same horizon-invariant variance $\sigma^2_{\mathfrak{s}}$, i.e. $\mathfrak{s}_{h,t} \sim N(0, \sigma^2_{\mathfrak{s}})$. We assume all rigidity parameters for distant horizons are the same as that of horizon $h = 12$. That is, we assume $\alpha_h = \alpha_{12}$ for $\forall h \geq 12$. Even imposing the restriction $\mathfrak{s}_{h,t} = 0$ for $\forall h \geq 14$, note that $\mathfrak{s}_{13,t}$ and $\mathfrak{s}_{12,t}$ are still affecting $\mathfrak{s}^{av}_{15,t}$. Therefore, $\mathfrak{s}_{13,t}$ and $\mathfrak{s}_{12,t}$ hit the dynamics of the non-observed forecast $\mathcal{F}_t\pi^{av}_{t+15}$. Since this forecast depends on the 3-month lagged value of the also non-observed forecast $\mathcal{F}_t\pi^{av}_{t+18}$, we proceed as follows. We let $\mathcal{F}_t\pi^{av}_{t+15}$ process be described by (8), while the dynamics of $\mathcal{F}_t\pi^{av}_{t+18}$ is described by (9).

Below, we show how those inference assumptions affect the estimated forecast system. Quarterly aggregation quantities, for $h \in \{-3, 0, 3, 6, 9, 12\}$ are $\mathcal{F}_t\pi^{av}_{t+h}$, $E^*_t\pi^{av}_{t+h}$ and $\mathfrak{s}_{h,t}$. Monthly aggregation quantities, for $j \in \{-6, ..., -2, -1, 0, 1, 2, ..., 18\}$, are $E^*_t\pi^{sa}_{t+j}$ and $E_{t-2}\pi^{sa}_{t+j}$.

$h = -6:$

$$E^*_t\pi^{sa}_{t-6} = \pi^{sa}_{t-6} \;\; ; \;\; E^*_t\pi^{sa}_{t-5} = \pi^{sa}_{t-5}$$

$h = -3:$

$$\begin{aligned}
\mathcal{F}_t\pi^{av}_{t-3} &= (1-\alpha_{-3})\, E^*_t\pi^{av}_{t-3} + \alpha_{-3}\mathcal{F}_{t-3}\pi^{av}_{t-3} \\
E^*_t\pi^{av}_{t-3} &= \tfrac{1}{3}\left[E^*_t\pi^{sa}_{t-2} + 2E^*_t\pi^{sa}_{t-3} + 3E^*_t\pi^{sa}_{t-4} + 2E^*_t\pi^{sa}_{t-5} + E^*_t\pi^{sa}_{t-6}\right] \\
E^*_t\pi^{sa}_{t-4} &= \pi^{sa}_{t-4} + \mathfrak{s}_{-3,t} \;\; ; \;\; E^*_t\pi^{sa}_{t-3} = \pi^{sa}_{t-3} + \mathfrak{s}_{-3,t} \;\; ; \;\; E^*_t\pi^{sa}_{t-2} = \pi^{sa}_{t-2} + \mathfrak{s}_{-3,t} \\
\mathfrak{s}_{-3,t} &\sim N\left(0, \sigma^2_{\mathfrak{s}}\right)
\end{aligned}$$

$h = 0:$

$$\begin{aligned}
\mathcal{F}_t\pi^{av}_{t} &= (1-\alpha_{0})\, E^*_t\pi^{av}_{t} + \alpha_{0}\mathcal{F}_{t-3}\pi^{av}_{t} \\
E^*_t\pi^{av}_{t} &= \tfrac{1}{3}\left[E^*_t\pi^{sa}_{t+1} + 2E^*_t\pi^{sa}_{t} + 3E^*_t\pi^{sa}_{t-1} + 2E^*_t\pi^{sa}_{t-2} + E^*_t\pi^{sa}_{t-3}\right] \\
E^*_t\pi^{sa}_{t+1} &= E_{t-2}\pi^{sa}_{t+1} + \mathfrak{s}_{0,t} \;\; ; \;\; E^*_t\pi^{sa}_{t} = E_{t-2}\pi^{sa}_{t} + \mathfrak{s}_{0,t} \;\; ; \;\; E^*_t\pi^{sa}_{t-1} = E_{t-2}\pi^{sa}_{t-1} + \mathfrak{s}_{0,t} \\
\mathfrak{s}_{0,t} &\sim N\left(0, \sigma^2_{\mathfrak{s}}\right)
\end{aligned}$$

$\vdots$

$h = 12:$

$$\begin{aligned}
\mathcal{F}_t\pi^{av}_{t+12} &= (1-\alpha_{12})\, E^*_t\pi^{av}_{t+12} + \alpha_{12}\mathcal{F}_{t-3}\pi^{av}_{t+12} \\
E^*_t\pi^{av}_{t+12} &= \tfrac{1}{3}\left[E^*_t\pi^{sa}_{t+13} + 2E^*_t\pi^{sa}_{t+12} + 3E^*_t\pi^{sa}_{t+11} + 2E^*_t\pi^{sa}_{t+10} + E^*_t\pi^{sa}_{t+9}\right] \\
E^*_t\pi^{sa}_{t+13} &= E_{t-2}\pi^{sa}_{t+13} + \mathfrak{s}_{12,t} \;\; ; \;\; E^*_t\pi^{sa}_{t+12} = E_{t-2}\pi^{sa}_{t+12} + \mathfrak{s}_{12,t} \\
E^*_t\pi^{sa}_{t+11} &= E_{t-2}\pi^{sa}_{t+11} + \mathfrak{s}_{12,t} \\
\mathfrak{s}_{12,t} &\sim N\left(0, \sigma^2_{\mathfrak{s}}\right)
\end{aligned}$$

$h = 15:$

$$\begin{aligned}
\mathcal{F}_t \pi^{av}_{t+15} &= (1-\alpha_{12}) E^*_t \pi^{av}_{t+15} + \alpha_{12} \mathcal{F}_{t-3} \pi^{av}_{t+15} \\
E^*_t \pi^{av}_{t+15} &= \tfrac{1}{3}\left[E^*_t \pi^{sa}_{t+16} + 2E^*_t \pi^{sa}_{t+15} + 3E^*_t \pi^{sa}_{t+14} + 2E^*_t \pi^{sa}_{t+13} + E^*_t \pi^{sa}_{t+12}\right] \\
E^*_t \pi^{sa}_{t+16} &= E_{t-2} \pi^{sa}_{t+16} \;\; ; \;\; E^*_t \pi^{sa}_{t+15} = E_{t-2} \pi^{sa}_{t+15} \;\; ; \;\; E^*_t \pi^{sa}_{t+14} = E_{t-2} \pi^{sa}_{t+14}
\end{aligned}$$

$h = 18:$

$$\begin{aligned}
\mathcal{F}_t \pi^{av}_{t+18} &= \mathcal{F}_t \pi^{amr.}_{t+18} + \mathcal{F}_t \pi^{asr}_{t+18} + \mathcal{F}_t \pi^{alr}_{t+18} \\
\mathcal{F}_t \pi^{amr.}_{t+18} &= (1-\alpha_{12}) E_{t-2} \pi^{amr}_{t+18} + \alpha_{12} (\rho_{mr})^3 \mathcal{F}_{t-3} \pi^{amr}_{t-3+18} \\
\mathcal{F}_t \pi^{asr.}_{t+18} &= (1-\alpha_{12}) E_{t-2} \pi^{asr}_{t+18} + \alpha_{12} (\rho_{sr})^3 \mathcal{F}_{t-3} \pi^{asr}_{t-3+18} \\
\mathcal{F}_t \pi^{alr}_{t+18} &= (1-\alpha_{12}) E_{t-2} \pi^{alr}_{t+18} + \alpha_{12} \mathcal{F}_{t-3} \pi^{alr}_{t-3+18}
\end{aligned}$$

$$\begin{aligned}
E_{t-2} \pi^{amr}_{t+18} &= \tfrac{1}{3} E_{t-2}\left[\pi^{mr}_{t+19} + 2\pi^{mr}_{t+18} + 3\pi^{mr}_{t+17} + 2\pi^{mr}_{t+16} + \pi^{mr}_{t+15}\right] \\
E_{t-2} \pi^{asr}_{t+18} &= \tfrac{1}{3} E_{t-2}\left[\pi^{sr}_{t+19} + 2\pi^{sr}_{t+18} + 3\pi^{sr}_{t+17} + 2\pi^{sr}_{t+16} + \pi^{sr}_{t+15}\right] \\
E_{t-2} \pi^{alr}_{t+18} &= \tfrac{1}{3} E_{t-2}\left[\pi^{lr}_{t+19} + 2\pi^{lr}_{t+18} + 3\pi^{lr}_{t+17} + 2\pi^{lr}_{t+16} + \pi^{lr}_{t+15}\right]
\end{aligned}$$

D Derivations for Forecast Dominance

Kalman recursion applied to this model implies $\mathcal{F}_{i,q} \pi^{av}_{q+1+\mathfrak{h}} = \rho_{\mathfrak{h}} \mathcal{F}_{i,q} \pi^{av}_{q+\mathfrak{h}}$ and $\mathcal{F}_q \pi^{av}_{q+1+\mathfrak{h}} = \rho_{\mathfrak{h}} \mathcal{F}_q \pi^{av}_{q+\mathfrak{h}}$. Therefore, using (10) and (11), the Individual Forecast error $\xi_{i,q,\mathfrak{h}} \equiv \mathcal{F}_{i,q} \pi^{av}_{q+\mathfrak{h}} - \pi^{av}_{q+\mathfrak{h}}$ satisfies:

$$\begin{aligned}
\xi_{i,q,\mathfrak{h}} = \;& \mathcal{F}_{i,q} \pi^{av}_{q+\mathfrak{h}} - \pi^{av}_{q+\mathfrak{h}} = \left(1-\gamma_{\mathfrak{h}}\right) \mathcal{F}_{i,q-1} \pi^{av}_{q+\mathfrak{h}} + \gamma_{\mathfrak{h}} E^*_{i,q} \pi^{av}_{q+\mathfrak{h}} - \pi^{av}_{q+\mathfrak{h}} \\
= \;& \left(1-\gamma_{\mathfrak{h}}\right) \rho_{\mathfrak{h}} \mathcal{F}_{i,q-1} \pi^{av}_{q+\mathfrak{h}-1} + \gamma_{\mathfrak{h}} \left(\pi^{av}_{q+\mathfrak{h}} + \eta_{\mathfrak{h},q+\mathfrak{h}} + \delta_{i,\mathfrak{h},q+\mathfrak{h}}\right) - \pi^{av}_{q+\mathfrak{h}} \\
= \;& \left(1-\gamma_{\mathfrak{h}}\right) \rho_{\mathfrak{h}} \mathcal{F}_{i,q-1} \pi^{av}_{q+\mathfrak{h}-1} - \left(1-\gamma_{\mathfrak{h}}\right) \pi^{av}_{q+\mathfrak{h}} + \gamma_{\mathfrak{h}} \left(\eta_{\mathfrak{h},q+\mathfrak{h}} + \delta_{i,\mathfrak{h},q+\mathfrak{h}}\right) \\
= \;& \left(1-\gamma_{\mathfrak{h}}\right) \left[\rho_{\mathfrak{h}} \mathcal{F}_{i,q-1} \pi^{av}_{q+\mathfrak{h}-1} - \pi^{av}_{q+\mathfrak{h}}\right] + \gamma_{\mathfrak{h}} \left(\eta_{\mathfrak{h},q+\mathfrak{h}} + \delta_{i,\mathfrak{h},q+\mathfrak{h}}\right) \\
= \;& \left(1-\gamma_{\mathfrak{h}}\right) \left[\rho_{\mathfrak{h}} \mathcal{F}_{i,q-1} \pi^{av}_{q+\mathfrak{h}-1} - \rho_{\mathfrak{h}} \pi^{av}_{q+\mathfrak{h}-1} - \varepsilon_{\mathfrak{h},q+\mathfrak{h}}\right] + \gamma_{\mathfrak{h}} \left(\eta_{\mathfrak{h},q+\mathfrak{h}} + \delta_{i,\mathfrak{h},q+\mathfrak{h}}\right) \\
= \;& \left(1-\gamma_{\mathfrak{h}}\right) \left(\rho_{\mathfrak{h}} \xi_{i,q-1,\mathfrak{h}} - \varepsilon_{\mathfrak{h},q+\mathfrak{h}}\right) + \gamma_{\mathfrak{h}} \left(\eta_{\mathfrak{h},q+\mathfrak{h}} + \delta_{i,\mathfrak{h},q+\mathfrak{h}}\right) \\
= \;& \left(1-\gamma_{\mathfrak{h}}\right) \rho_{\mathfrak{h}} \xi_{i,q-1,\mathfrak{h}} - \left(1-\gamma_{\mathfrak{h}}\right) \varepsilon_{\mathfrak{h},q+\mathfrak{h}} + \gamma_{\mathfrak{h}} \upsilon_{i,\mathfrak{h},q+\mathfrak{h}}
\end{aligned}$$

Since the Average Forecast error satisfies $\xi_{q,\mathfrak{h}} \equiv \int_0^1 \xi_{i,q,\mathfrak{h}} di$, and $\int_0^1 \upsilon_{i,\mathfrak{h},q+\mathfrak{h}} di = \eta_{\mathfrak{h},q+\mathfrak{h}}$, we obtain $\xi_{q,\mathfrak{h}} = \left(1-\gamma_{\mathfrak{h}}\right) \rho_{\mathfrak{h}} \xi_{q-1,\mathfrak{h}} - \left(1-\gamma_{\mathfrak{h}}\right) \varepsilon_{\mathfrak{h},q+\mathfrak{h}} + \gamma_{\mathfrak{h}} \eta_{\mathfrak{h},q+\mathfrak{h}}$. And lastly, since $E^*_q \pi^{av}_{q+\mathfrak{h}} = \pi^{av}_{q+\mathfrak{h}} + \eta_{\mathfrak{h},q+\mathfrak{h}}$, the Resetting Forecast error is $\xi^*_{q,\mathfrak{h}} \equiv E^*_q \pi^{av}_{q+\mathfrak{h}} - \pi^{av}_{q+\mathfrak{h}} = \eta_{\mathfrak{h},q+\mathfrak{h}}$.

As for Proposition 2, the proof is shown below.

Proposition 2 *Consider the modelling assumptions and results presented in Sections 5.1 and 5.2. In this case, the Resetting Forecast $E_q^* \pi_{q+\mathfrak{h}}^{av}$ has better forecasting performance than the Average Forecast $F_q \pi_{q+\mathfrak{h}}^{av}$ if and only if disagreement $\frac{\vartheta_{i,\mathfrak{h}}}{\vartheta_{\mathfrak{h}}}$ satisfies the following condition:*

$$\frac{2}{\left[1 + (\bar{\sigma}^2/\vartheta_{\mathfrak{h}})^{-1}\right]} < \frac{\vartheta_{i,\mathfrak{h}}}{\vartheta_{\mathfrak{h}}} < \frac{\bar{\sigma}^2}{\vartheta_{\mathfrak{h}}}$$

Proof. From Kalman recursion, we have:

$$\gamma_{\mathfrak{h}} = \frac{\kappa_{\mathfrak{h}} \bar{\sigma}^2}{\kappa_{\mathfrak{h}} \bar{\sigma}^2 + \sigma_{\upsilon,\mathfrak{h}}^2} \quad ; \; \kappa_{\mathfrak{h}} = \frac{\left(1 - \left(\rho_{\mathfrak{h}}\right)^2\right)}{2} \left[\left(1 - \frac{\sigma_{\upsilon,\mathfrak{h}}^2}{\bar{\sigma}^2}\right) + \sqrt{\left(1 - \frac{\sigma_{\upsilon,\mathfrak{h}}^2}{\bar{\sigma}^2}\right)^2 + \frac{4}{\left(1 - \left(\rho_{\mathfrak{h}}\right)^2\right)} \frac{\sigma_{\upsilon,\mathfrak{h}}^2}{\bar{\sigma}^2}} \right]$$

Therefore, we obtain:

$$\kappa_{\mathfrak{h}} = \frac{\left(1 - \left(\rho_{\mathfrak{h}}\right)^2\right)}{2} \left[\left(1 - \frac{\sigma_{\upsilon,\mathfrak{h}}^2}{\bar{\sigma}^2}\right) + \sqrt{\left(1 - \frac{\sigma_{\upsilon,\mathfrak{h}}^2}{\bar{\sigma}^2}\right)^2 + \frac{4}{\left(1 - \left(\rho_{\mathfrak{h}}\right)^2\right)} \frac{\sigma_{\upsilon,\mathfrak{h}}^2}{\bar{\sigma}^2}} \right] = \frac{\gamma_{\mathfrak{h}}}{\left(1 - \gamma_{\mathfrak{h}}\right)} \frac{\sigma_{\upsilon,\mathfrak{h}}^2}{\bar{\sigma}^2}$$

It implies that

$$\sqrt{\left(1 - \frac{\sigma_{\upsilon,\mathfrak{h}}^2}{\bar{\sigma}^2}\right)^2 + \frac{4}{\left(1 - \left(\rho_{\mathfrak{h}}\right)^2\right)} \frac{\sigma_{\upsilon,\mathfrak{h}}^2}{\bar{\sigma}^2}} = \left[\frac{2\gamma_{\mathfrak{h}}}{\left(1 - \left(\rho_{\mathfrak{h}}\right)^2\right)\left(1 - \gamma_{\mathfrak{h}}\right)} + 1 \right] \frac{\sigma_{\upsilon,\mathfrak{h}}^2}{\bar{\sigma}^2} - 1$$
$$\therefore \left(1 - \frac{\sigma_{\upsilon,\mathfrak{h}}^2}{\bar{\sigma}^2}\right)^2 + \frac{4}{\left(1 - \left(\rho_{\mathfrak{h}}\right)^2\right)} \frac{\sigma_{\upsilon,\mathfrak{h}}^2}{\bar{\sigma}^2} = \left(\left[\frac{2\gamma_{\mathfrak{h}}}{\left(1 - \left(\rho_{\mathfrak{h}}\right)^2\right)\left(1 - \gamma_{\mathfrak{h}}\right)} + 1 \right] \frac{\sigma_{\upsilon,\mathfrak{h}}^2}{\bar{\sigma}^2} - 1 \right)^2$$

$$\therefore \bar{\sigma}^2 = \gamma_{\mathfrak{h}} \left[\frac{\gamma_{\mathfrak{h}}}{\left(1 - \left(\rho_{\mathfrak{h}}\right)^2\right)\left(1 - \gamma_{\mathfrak{h}}\right)} + 1 \right] \sigma_{\upsilon,\mathfrak{h}}^2 \tag{14}$$

From (12), we have:

$$\vartheta_{i,\mathfrak{h}} = \frac{\left(1 - \gamma_{\mathfrak{h}}\right)^2 \sigma_{\mathfrak{h}}^2 + \left(\gamma_{\mathfrak{h}}\right)^2 \sigma_{\upsilon,\mathfrak{h}}^2}{1 - \left(1 - \gamma_{\mathfrak{h}}\right)^2 \rho_{\mathfrak{h}}^2} \quad ; \; \vartheta_{\mathfrak{h}} = \frac{\left(1 - \gamma_{\mathfrak{h}}\right)^2 \sigma_{\mathfrak{h}}^2 + \left(\gamma_{\mathfrak{h}}\right)^2 \sigma_{\eta,\mathfrak{h}}^2}{1 - \left(1 - \gamma_{\mathfrak{h}}\right)^2 \rho_{\mathfrak{h}}^2} \quad ; \; \vartheta_{\mathfrak{h}}^* = \sigma_{\eta,\mathfrak{h}}^2$$

Using the expression for $\vartheta_{i,\mathfrak{h}}$, and recalling that $\sigma_{\mathfrak{h}}^2 = \left(1 - \left(\rho_{\mathfrak{h}}\right)^2\right) \bar{\sigma}^2$, we obtain:

$$\left[1 - \left(1 - \gamma_{\mathfrak{h}}\right)^2 \rho_{\mathfrak{h}}^2\right] \vartheta_{i,\mathfrak{h}} = \left(1 - \gamma_{\mathfrak{h}}\right)^2 \left(1 - \left(\rho_{\mathfrak{h}}\right)^2\right) \gamma_{\mathfrak{h}} \left[\frac{\gamma_{\mathfrak{h}}}{\left(1 - \left(\rho_{\mathfrak{h}}\right)^2\right)\left(1 - \gamma_{\mathfrak{h}}\right)} + 1 \right] \sigma_{\upsilon,\mathfrak{h}}^2 + \left(\gamma_{\mathfrak{h}}\right)^2 \sigma_{\upsilon,\mathfrak{h}}^2$$

$$\therefore \sigma_{\upsilon,\mathfrak{h}}^2 = \frac{1}{\gamma_{\mathfrak{h}}} \vartheta_{i,\mathfrak{h}} \tag{15}$$

And so, plugging the previous result for $\sigma^2_{\upsilon,\mathfrak{h}}$ into (14), we obtain:

$$\left(\rho_{\mathfrak{h}}\right)^2 = 1 - \frac{\gamma_{\mathfrak{h}}}{\left(1-\gamma_{\mathfrak{h}}\right)\left(\frac{\bar{\sigma}^2}{\vartheta_{i,\mathfrak{h}}}-1\right)} \tag{16}$$

Using the expressions for $\vartheta_{\mathfrak{h}}$ and $\left(\rho_{\mathfrak{h}}\right)^2$, and recalling that $\sigma^2_{\mathfrak{h}} = \left(1-\left(\rho_{\mathfrak{h}}\right)^2\right)\bar{\sigma}^2$, we obtain:

$$\begin{aligned}
\sigma^2_{\eta,\mathfrak{h}} &= \frac{1}{\left(\gamma_{\mathfrak{h}}\right)^2}\left[1-\left(1-\gamma_{\mathfrak{h}}\right)^2\rho^2_{\mathfrak{h}}\right]\vartheta_{\mathfrak{h}} - \frac{\left(1-\gamma_{\mathfrak{h}}\right)^2}{\left(\gamma_{\mathfrak{h}}\right)^2}\left(1-\left(\rho_{\mathfrak{h}}\right)^2\right)\bar{\sigma}^2 \\
&= \frac{1}{\left(\gamma_{\mathfrak{h}}\right)^2}\left[1-\left(1-\gamma_{\mathfrak{h}}\right)^2+\frac{\left(1-\gamma_{\mathfrak{h}}\right)\gamma_{\mathfrak{h}}}{\left(\frac{\bar{\sigma}^2}{\vartheta_{i,\mathfrak{h}}}-1\right)}\right]\vartheta_{\mathfrak{h}} - \frac{\left(1-\gamma_{\mathfrak{h}}\right)}{\gamma_{\mathfrak{h}}\left(\frac{\bar{\sigma}^2}{\vartheta_{i,\mathfrak{h}}}-1\right)}\bar{\sigma}^2 \\
&= \frac{1}{\left(\frac{\bar{\sigma}^2}{\vartheta_{i,\mathfrak{h}}}-1\right)}\left[\left(\frac{\left(2-\gamma_{\mathfrak{h}}\right)}{\gamma_{\mathfrak{h}}}\frac{\bar{\sigma}^2}{\vartheta_{i,\mathfrak{h}}}-\frac{1}{\gamma_{\mathfrak{h}}}\right)\vartheta_{\mathfrak{h}} - \frac{\left(1-\gamma_{\mathfrak{h}}\right)}{\gamma_{\mathfrak{h}}}\bar{\sigma}^2\right]
\end{aligned}$$

If Resetting Forecast has better forecasting performance than the Average Forecast, then $\vartheta^*_{\mathfrak{h}} < \vartheta_{\mathfrak{h}}$. Since $\vartheta^*_{\mathfrak{h}} = \sigma^2_{\eta,\mathfrak{h}}$, it is equivalent to:

$$\frac{1}{\left(\frac{\bar{\sigma}^2}{\vartheta_{i,\mathfrak{h}}}-1\right)}\left[\left(\frac{\left(2-\gamma_{\mathfrak{h}}\right)}{\gamma_{\mathfrak{h}}}\frac{\bar{\sigma}^2}{\vartheta_{i,\mathfrak{h}}}-\frac{1}{\gamma_{\mathfrak{h}}}\right)\vartheta_{\mathfrak{h}} - \frac{\left(1-\gamma_{\mathfrak{h}}\right)}{\gamma_{\mathfrak{h}}}\bar{\sigma}^2\right] < \vartheta_{\mathfrak{h}}$$

Moreover, since $\left(\rho_{\mathfrak{h}}\right)^2 < 1$, equation (16) implies that $\left(\frac{\bar{\sigma}^2}{\vartheta_{i,\mathfrak{h}}}-1\right) > 0$. Therefore, the previous inequality can be written as follows:

$$\begin{aligned}
&\left[\frac{\left(2-\gamma_{\mathfrak{h}}\right)}{\gamma_{\mathfrak{h}}}\frac{\bar{\sigma}^2}{\vartheta_{i,\mathfrak{h}}}-\frac{1}{\gamma_{\mathfrak{h}}}\right]\vartheta_{\mathfrak{h}} - \frac{\left(1-\gamma_{\mathfrak{h}}\right)}{\gamma_{\mathfrak{h}}}\bar{\sigma}^2 < \left(\frac{\bar{\sigma}^2}{\vartheta_{i,\mathfrak{h}}}-1\right)\vartheta_{\mathfrak{h}} \;\therefore\; \left[\frac{2\left(1-\gamma_{\mathfrak{h}}\right)}{\gamma_{\mathfrak{h}}}\frac{\bar{\sigma}^2}{\vartheta_{i,\mathfrak{h}}}-\frac{\left(1-\gamma_{\mathfrak{h}}\right)}{\gamma_{\mathfrak{h}}}\right]\vartheta_{\mathfrak{h}} - \frac{\left(1-\gamma_{\mathfrak{h}}\right)}{\gamma_{\mathfrak{h}}}\bar{\sigma}^2 < 0 \\
&\therefore \left(2\frac{\bar{\sigma}^2}{\vartheta_{i,\mathfrak{h}}}-1\right)\vartheta_{\mathfrak{h}} - \bar{\sigma}^2 < 0 \;\therefore\; 2 < \vartheta_{i,\mathfrak{h}}\left(\frac{1}{\vartheta_{\mathfrak{h}}}+\frac{1}{\bar{\sigma}^2}\right) \;\therefore\; 2 < \frac{\vartheta_{i,\mathfrak{h}}}{\vartheta_{\mathfrak{h}}}\frac{\left(\bar{\sigma}^2+\vartheta_{\mathfrak{h}}\right)}{\bar{\sigma}^2} \\
&\therefore \frac{2\bar{\sigma}^2}{\left(\bar{\sigma}^2+\vartheta_{\mathfrak{h}}\right)} < \frac{\vartheta_{i,\mathfrak{h}}}{\vartheta_{\mathfrak{h}}}
\end{aligned}$$

Moreover, dividing by $\vartheta_{\mathfrak{h}}$, the inequality $\left(\frac{\bar{\sigma}^2}{\vartheta_{i,\mathfrak{h}}}-1\right) > 0$ can be rewritten as $\frac{\vartheta_{i,\mathfrak{h}}}{\vartheta_{\mathfrak{h}}} < \frac{\bar{\sigma}^2}{\vartheta_{\mathfrak{h}}}$. Therefore, we obtain the following condition:

$$\frac{2}{\left[1+\left(\bar{\sigma}^2/\vartheta_{\mathfrak{h}}\right)^{-1}\right]} < \frac{\vartheta_{i,\mathfrak{h}}}{\vartheta_{\mathfrak{h}}} < \frac{\bar{\sigma}^2}{\vartheta_{\mathfrak{h}}}$$

■